An Experimental Investigation of Heat Transfer in the Thermally Developing Region of a Pulsating Pipe Flow

by

Semiu Adesina Gbadebo

A Thesis Presented to the

FACULTY OF THE COLLEGE OF GRADUATE STUDIES

KING FAHD UNIVERSITY OF PETROLEUM & MINERALS

DHAHRAN, SAUDI ARABIA

In Partial Fulfillment of the
Requirements for the Degree of

MASTER OF SCIENCE

In

MECHANICAL ENGINEERING

December, 1996

AN EXPERIMENTAL INVESTIGATION OF HEAT TRANSFER IN THE THERMALLY DEVELOPING REGION OF A PULSATING PIPE FLOW

BY

SEMIU ADESINA GBADEBO

A Thesis Presented to the

FACULTY OF THE COLLEGE OF GRADUATE STUDIES

KING FAHD UNIVERSITY OF PETROLEUM & MINERALS

DHAHRAN, SAUDI ARABIA

In Partial Fulfillment of the
Requirements for the Degree of

MASTER OF SCIENCE

In

MECHANICAL ENGINEERING

DECEMBER, 1996

UMI Number: 1385308

UMI
300 North Zeeb Road
Ann Arbor, MI 48103

KING FAHD UNIVERSITY OF PETROLEUM AND MINERALS
DHAHRAN 31261, SAUDI ARABIA

COLLEGE OF GRADUATE STUDIES

This thesis, written by ***GBADEBO SEMIU ADESINA*** *under the direction of his Thesis Advisor and approved by his Thesis Committee, has been presented to and accepted by the Dean of the College of Graduate Studies, in partial fulfillment of the requirements for the degree of* ***MASTER OF SCIENCE*** *in Mechanical Engineering.*

Thesis Committee

Dr. Abdul-Ghani Al-Farayedhi
(Chairman)

Dr. S.A.M Said
(Co-Chairman)

Dr. Muhammed Habib

Dr. Saad Ahmed

Dr. M.O Budair
Chairman, Mechanical Engineering Dept.

Dr. Abdullah M. Al-Shehri
Dean, College of Graduate Studies

28/4/97
DATE

DEDICATION

To my Parents

and to

Ruqaya, Mohammed Sadiq and AbdulHakeem

ACKNOWLEDGMENT

In the name of Allah , Most Gracious, Most Merciful

' Of knowledge, It is only a little that is communicated to you (O' men!)' (Qur'an 17: 85)

My deepest appreciation goes to my thesis advisor, Dr. Abdul Ghani Al-Farayedhi, for his invaluable help, suggestions, and encouragement throughout this work. I am greatly indebted to my co-advisor, Dr. S.A.M. Said for his endless support, constructive criticisms and guidance.

Many thanks are due to my thesis committee members, Dr. Mohammed Habib for his vision and encouragement and Dr. Saad Ahmed for his cooperation and advice.

I would like to express my sincere appreciation to the entire community of King Fahd University of Petroleum and Minerals for greatly supporting this work, being part of the University funded project by providing all literature, necessary facilities and equipment. I would like to thank Messrs: Asad Asghar and Salem Al-Dini for their assistance and support throughout this work. My deep appreciation also goes to the Mechanical Engineering workshop for the construction of the test rig under the supervision of Mr. Kamal Ali.

Appreciation also goes to the chairman of Mechanical Engineering Department, Dr. M.O. Budair and the entire faculty, staff and students for their cooperation and support.

I would also like to acknowledge my family for their patience, encouragement and understanding while carrying out this work.

TABLE OF CONTENTS

LIST OF TABLES

LIST OF FIGURES

THESIS ABSTRACT

NAME OF STUDENT : GBADEBO, SEMIU ADESINA

TITLE OF STUDY : AN EXPERIMENTAL INVESTIGATION OF HEAT TRANSFER IN THE THERMALLY DEVELOPING REGION OF A PULSATING PIPE FLOW

MAJOR FIELD : MECHANICAL ENGINEERING

DATE OF DEGREE : DECEMBER, 1996

The effect of pulsation on heat transfer coefficient in the thermally developing region of turbulent air flow in a pipe was investigated. The pipe wall was electrically heated to provide uniform heat flux. Reynolds number was varied from 6387 to 41947 while frequencies of pulsation ranged from 1 to 13 Hz in an almost sinusoidal form. The displacement amplitude of pulsation inducing mechanism was kept constant throughout the experiment. The behavior of local Nusselt number under the influence of pulsation was studied. The results show enhancement in the mean Nusselt number up to 9 % at frequency of 2 Hz for Reynolds number of about 15000. The rate of enhancement decreases as Re increases and the frequency band at which enhancement is observed widens and lies between 1.5 and 3.5 Hz for Re between 15000 and 33000. Reduction of heat transfer coefficient is encountered at higher frequencies and the effect of pulsation becomes insignificant as Re becomes very high. It can be concluded that the effect of pulsation on the heat transfer coefficient is less significant in the thermally developing region of turbulent air flow in pipes. This may be due to the already high heat transfer coefficient which exists in this region of developing thermal boundary layer.

ملخص بحث

الاسم : سميع أديسينا باديبو

العنوان : الكشف التجريبي عن انتقال الحرارة في منطقة التطور الحراري لانبوب متعرض لتيار نابض

الدرجة : ماجستير

التخصص : هندسة ميكانيكية

التاريخ : ديسمبر ١٩٩٦

تم فحص أثر النبضان على مكافيء انتقال الحرارة في منطقة التطور الحراري لسريان هواء مضطرب عند مدخل انبوب . وقد تم تسخين الانبوب كهربائيا لتوليد فيض حراري منتظم . وقد تفاوتت أرقام رينولدز بين ٦٣٨٧ و ٤١٩٤٧ في حين أن النبضان تراوح بين ١ و ١٣ هيرتز وفي شكل منحنى جيبي تقريبا .وظل متسع ذبذبة النبضان الناتج عن جهاز توليد النبضان ثابتا طوال مدة التجربة .ولقد تمت دراسة النبضان على رقم نسلت المحلي . وأظهرت النتائج تحسنا لمتوسط رقم نسلت بمعدل ٩ ٪ عند ذبذبة ٢ هيرتز لرقم رينولدز ١٥٠٠٠ . وكما لوحظ أن معدل التحسن ينخفض عند زيادة ارقام رينولدز ، وأن مجال التردد التي تم ملاحظة التحسن عنده يتغير بين ٥ر١ الى ٥ر٣ هيرتز لأرقام رينولدز ، وكما لوحظ أن معدل التحسن ينخفض عند زيادة ارقام رينولور من ١٥٠٠ الى ٣٣٠٠٠ في مجال تردد يتغير من ٥ر١ الى ٥ر٣ هيرتز . ولوحظ انخفاض مكافيء انتقال الحرارة عند ذبذبات النبضان العليا وأن أثر النبضان يصبح غير مؤثر مع شدة ازدياد أرقام رينولدز . ويمكن التلخيص بأن أثر النبضان على مكافئ انتقال الحرارة يكون أقل أثرا في منطقة التطور الحراري للهواء المضطرب داخل انبوب . وقد يعزى ذلك الى ارتفاع معدل مكافيء انتقال الحرارة الموجود أصلا في منطقة التطور الحراري .

درجة الماجستير في العلوم

جامعة الملك فهد للبترول والمعادن

الظهران – المملكة العربية السعودية

ديسمبر ١٩٩٦م

CHAPTER 1

INTRODUCTION

1.1 Background

The rapid technological development in modern power industries, heat, chemical and other branches of industrial engineering has called for an in-depth study of hydrodynamic and thermal process that take place in unsteady turbulent flows. One of such flows that frequently occur in practice is a pulsating flow. This flow is characterized by periodic fluctuation of the mass flow rate. This definition implies a base flow rate on which some perturbations are imposed. [1]. Attempts to establish numerical and analytical solutions to problems of hydrodynamics and heat transfer in pulsating flows have been posed with difficulties due to the complicated nature of unsteady turbulent flows. Experimental investigation of pulsating flows has therefore been the most reliable way of understanding this phenomenon.

The hydrodynamics of pulsating flows has been extensively studied and many of its related aspects are now clearly understood. However, the heat transfer characteristics of pulsating flows have not been fully established. Due to a variety of control parameters (such as pulsation frequency, amplitude,

wave-form and location of pulsator relative to the flow), previous researchers showed conflicting findings for the effect of pulsation on heat transfer. As far as pulsating pipe flow is concerned, available experimental data on the heat transfer characteristics have been inconclusive. Some investigators reported heat transfer enhancement with a pulsating flow [2 ,3] whereas, reduction in heat transfer were noted by others [4]. In some cases, both increase and reduction were recorded in a single experiment at different flow conditions [5].

The inconclusive and conflicting nature of the previous work on pulsating internal flows has thus prompted the present work. Perusal of literature on this subject shows that no extensive experimental work has been carried out regarding the effect of pulsation on heat transfer characteristics in the thermally developing region of turbulent pipe flow.

Thermal entrance length is defined as the heated pipe length required to achieve a local value of heat transfer coefficient or Nusselt number equal to about 1.05 times the fully developed value [6 , 7]. Generally, the thermal entrance length of turbulent flow in pipes ranges from 10 to 15 diameters [8]. In particular, thermal entrance length for turbulent air flow in pipes is about 12 pipe diameters and is independent of the magnitude of flow Reynolds number as investigated by **Babus'haq** [6].

1.2 Engineering Applications

There are many types of flow which are pulsating in nature. These types of flow associated with heat transfer have relevant engineering applications. The followings are typical examples:

1. Flows at inlet and exhaust ducts of reciprocating engines such as the internal combustion engines.
2. Flows in which the fluid is pumped by centrifugal or reciprocating devices such as discharge of piston and gear pumps. Pulsation also arises in flows in hydraulic or pneumatic lines of control systems.
3. Flow in systems whose operation is based on the wave action such as the pulse - jet.
4. In the field of pulmonary physiology, blood circulation is another typical pulsed flow where the heat exchange between the blood and tissues could be influenced by pulsation. In general flows in most biological systems are pulsating, perhaps due to the wide use of peristaltic pumps in cardiovascular flow dynamics and measurements [9].

1.3 Research Objectives

The main objective of this research work is to investigate heat transfer characteristics in pulsating internal flows with particular attention to the effect of pulsation on average heat transfer coefficient in the thermal entrance

region of a turbulent pulsating pipe flow using air as working fluid. In order to accomplish this objective, an experimental set-up is built.

1.4 Scope of the Present Work

Effect of pulsation on heat transfer coefficient in the thermal entrance region of a hydrodynamically fully developed turbulent pipe flow of air was investigated. It is one of the series of experiments designed with a view to fully understanding this phenomenon with varied geometries. So far there has not been any reported extensive experimental investigation on the effect of pulsation on the heat transfer coefficient in the thermal entrance region of turbulent flow in pipes. In this work, a total of 55 tests were carried out and each flow pulsation was preceded by the corresponding steady flow without pulsation at the same flow Reynolds number. The flow is assumed to be incompressible and fluid properties are assumed constant in the range of flow temperatures considered. The flow Reynolds number was varied between 6387 and 41947 while frequencies of pulsation ranged from 1 Hz to 13 Hz in an almost sinusoidal form. Displacement amplitude of the pulsation inducing mechanism was kept constant at 0.025 m throughout the experiment.

CHAPTER 2

LITERATURE SURVEY

2.1 Introduction

This chapter is devoted primarily to the review of previous research work on heat transfer in pulsating flows as well as hydrodynamic studies on effect of pulsation on velocity and pressure distribution. Also, other reported methods identified for heat transfer enhancement as well as predictive turbulence models for pulsating flows are reviewed.

2.2 Heat Transfer in Pulsating Flows

Investigation of heat transfer in pulsating internal flows have been carried out both experimentally and theoretically. However, due to complicated nature of the flow, analytical and numerical solutions are only available to pulsating laminar flows. A number of these investigations are reviewed below:

2.2.1 Experimental Investigation

The earliest work on heat transfer characteristics of pulsating flow was carried out in 1943 by **Martinelli et al.** [10]. They investigated the heat

transfer in a semi-sinusoidal flow of water which is pumped by a reciprocating pump to a 0.0107 m. diameter vertical tube, steam heated to provide uniform wall temperature. Reynolds number was varied from 2000 to 77000 while the oscillating frequency ranged from 0.2167 Hz to 4.4167 Hz. Within this requency range, Nusselt number was found practically unaffected. However in the turbulent flow regime, It was slightly higher than the steady flow value at low Reynolds numbers (Re < 4500) while it was slightly lower at Re > 4500.

West and Taylor [2], studied the effect of partially damped pulsations from a reciprocating pump, on heat transfer coefficient of water in a 0.0508 m. diameter, 6.0 m. long, horizontal tube of a heat exchanger. Reynolds number was varied from 30000 to 85000. An increase between 60 % and 70 % in the heat transfer coefficient was recorded at 1.6 Hz.

Haveman and Rao [11] investigated the effect of pulsation on steam heated air flowing near atmospheric pressure in a horizontal pipe of 0.0254 m. diameter and 2.083 m. effective length. Pulsation was produced by means of a puppet valve operating in the path of the flow. Reynolds number was varied between 5000 and 35000 while their pulsation frequency was between 5 Hz and 33 Hz. It was found that Nu changed up to about 30 % under different conditions of frequency, amplitude, wave form and Re. The change was negative below certain frequency and positive above it. A very negligible change was found when amplitude was very low while at higher amplitude,

change in Nusselt number was found to be a function of amplitude, frequency and Reynolds number.

Lemlich [12] investigated the effect of pulsation on heat transfer coefficient of water in a 0.0127 m. diameter, 0.9144 m. long copper double pipe, steam to water heat exchanger. An electrical-hydraulic pulsator consisting of a solenoid valve triggered by an adjustable pressure switch was employed. Pulsation frequency of 1.5 Hz was attained and Reynolds number was varied from 2000 to 20000. The imposed pulsation increased the overall heat transfer coefficient up to about 80 % at Re = 2000 when the solenoid valve was located upstream.

Effect of acoustic vibration on heat transfer coefficient of air, flowing in the core of a horizontal, double pipe steam-to-air heat exchanger was studied by **Lemlich and Hwu** [13]. Flow Reynolds number was varied between 560 and 5900. The sound vibration frequency ranged between 180 Hz and 340 Hz and was introduced by an electromagnetic driver, actuated through an audio amplifier by variable sinusoidal audio signal generator. The result showed increase of about 51% in Nu in the nominally laminar regime and up to 27% in the nominally turbulent regime.

In another experiment carried out by **Baird et al.** [14], cold water was passed upward through a steam jacketed copper tube of 0.01905 m. diameter, heat transfer area of 0.05546 m^2 and approximately 0.9144 m. long. Sinusoidal pulsations were produced by air pulser consisting of an injection and exhaust

valve operated by a balsa-wood float and connected to a glass tube. Frequency of pulsation ranged from 0.8 Hz to 1.7 Hz while pulsation amplitude in the heat exchange tube varied from 0.0274 to 0.335 m. Reynolds number was between 4300 and 16200. Their result showed maximum enhancement of about 41% based on the overall heat transfer coefficient for Re less than 8000

Mamayev et al. [5] studied the effect of pulsation frequency on air, flowing in a stainless vertical tube of internal diameter of 0.008m. and 0.8m length, using constant heat flux. Reynolds number was varied between 540 and 11000 while the frequency of pulsation ranged from 0.5 Hz to 24.0 Hz. The pulsator, located downstream of the flow, consisted of a magnetic valve driven by a D.C motor through a rigid pool rod. The result showed that for laminar flow at $f \leq 2.0$ Hz, relative heat transfer coefficient decreased but it increased for $f \geq 5.0$ Hz. However, it increased all through in the turbulent flow regime up till 14.0 Hz with maximum increase of about 44 % at 12.0 Hz. For frequencies greater than 20.0 Hz, pulsation was found to have negative effect on the heat transfer coefficient.

Liao and Wang [4] also studied the effect of pulsation on heat transfer coefficient of turbulent, fully developed and steady pulsating flow of water in a stainless steel tube of 0.01092 m diameter and 1.96 m length. Flow pulsation was introduced using a motor driven ball valve system. Reynolds number ranged from 3400 to 27000 while pulsation frequency was varied between 0.074 Hz. and 0.38 Hz.. Their result showed about 20 % reduction in the heat

transfer coefficient with pulsation without flow reversal and the magnitude of the reduction was found to depend on amplitude. However, with flow reversal, there was almost a 25 % increase in the heat transfer coefficient.

Karamercan and Gainer [3] studied the effect of pulsation on water flowing in two double pipe heat exchangers of length 1.83 m and 0.914 m respectively, with steam on the shell side. The heat exchangers are both made of copper tube and stainless steel outer shell with inside diameters of 0.019 m and 0.0572 m respectively. Pulsation was generated by a reciprocating pump and frequencies ranged up to 5 Hz while Reynolds number was varied from 1000 to 50000. Five displacement amplitudes which could be made large enough to cause flow reversal were used at each frequency and Re. Their result showed considerable enhancement of heat transfer coefficient as amplitude increases resulting to low flow reversal frequencies. Also greater enhancement was recorded when the pulsator was located up stream.

Genin et al. [15] also studied the effect of pulsation on heat transfer coefficient of water flowing in a thin walled stainless steel tube of 0.029 m. diameter which was electrically heated to provide a uniform heat flux. Reynolds number was varied between 2000 and 25000 while pulsation frequency ranged from 0.2 Hz to 6 Hz. It was found that the nature of heat transfer along the test section with pulsating flow rate was no different from the distribution with constant flow rate. However, the relative mean Nusselt number ($Nu_{pulsation} / Nu_{steady}$) showed a tendency towards a drop in heat transfer in that

range of pulsation frequencies and on the overall, produces no significant effect on heat transfer coefficient.

Another experiment on the prediction of heat transfer coefficient in pulsating flow was carried out by **Al-Haddad and Al-Binally** [16]. Here, a furnace was used to heat air, subjected to convective cooling along a 2.0 m long, 0.127 m. diameter copper pipe. The air velocity was measured with anemometer while flow pulsation was introduced by a piston and cylinder, located upstream and connected to an electric driven motor with variable voltage. Reynolds number ranged between 1000 and 40000 while pulsation frequencies varied from 5.0 Hz to 60.0 Hz in a sine form. Fluid temperatures were measured at center line of the pipe at all sections. A combined dimensionless number $(Re\,\omega^*)$ was used to develop empirical correlation for Nusselt number given as:

$$Nu = Pr^{0.3}\left[23 + \frac{5.6\left(Re\,\omega^* \times 10^{-5} - 2\right)^2}{1 + 0.17\left(Re\,\omega^* \times 10^{-5} - 2\right)}\right] \qquad \textbf{(2.1)}$$

A critical value of this dimensionless number (of about 2.1×10^5) was noticed below which there was no improvement in Nu and above which Nu increased asymptotically.

Isshiki et al. [17] carried out an experimental investigation on the effect of pulsation on heat transfer in fully developed turbulent air flow in a 0.0476 m. diameter stainless steel pipe electrically heated to provide uniform wall heat flux.

A blower, located downstream was used to suck in air through a bellmouth to the velocity development section that varied between 32 to 116 diameters and through temperature development section of 2.45 m. and test section of 0.35m lengths respectively. Flow pulsation was generated by rotating a 1.0 mm. thick circular vane attached to a 5.0 mm. diameter axis located perpendicularly in the pipe and downstream after the test section. The mean velocities and turbulent intensities were measured using hot and cold wire technique at time-averaged Reynolds number of about 7450 while pulsation frequencies were in the ratio of 0.32, 0.61, 1.7 and 3.3 to the turbulent bursting frequency. This is defined as the frequency of occurrence of (series of periodic) activities that take place at the edge of the inner layer of turbulent boundary layer and was measured to be 9.73 Hz. Their results showed no change in the time averaged turbulent intensities and temperature field near the wall. The Nusselt number was found to vary periodically at lower pulsating frequencies than the bursting frequency while it is unchanged at higher frequencies.

The summary of previous experimental work on heat transfer in pulsating flows and the trend of findings is shown in Table 2.1

2.2.2 Analytical and Numerical Studies

Siegel and Perlmutter [18] in an analytical study of both laminar thermal entrance and fully developed pulsating channel flows introduced flow pulsation

Table 2.1 Summary of previous experimental work on heat transfer in pulsating flows

Date	Investigators	Nature of flow	Operating parameters	Results
1943	Martinelli et al. [10]	Heated water	$2000 \leq Re \leq 77000$ $0.217 \leq f \leq 4.417$Hz	No significant change in Nu
1952	West and Taylor [2]	Heated water	$30000 \leq Re \leq 85000$ $f = 1.67$ Hz $1.0 \leq A_r \leq 1.56$	Increase of 60 to 70% in Nu at f as A_r increases.
1954	Haveman and Rao [11]	Heated air	$5000 \leq Re \leq 35000$ $5 \leq f \leq 33$Hz	Nu changed up to 30% . Increase above a certain f and a decrease below it
1961	Lemlich R. [12]	Heated water	$2000 \leq Re \leq 20000$ $0 \leq f \leq 1.5$Hz	Increase of 80% in Nu at Re= 2000
1961	Lemlich and Hwu [13]	Heated air	$560 \leq Re \leq 5900$ $180 \leq f \leq 340$ Hz	Increase of 51% in Nu in laminar & up to 27% in the turbulent regime
1966	Baird et al. [14]	Heated water	$4300 \leq Re \leq 16200$ $0.7 \leq f \leq 1.7$ Hz $0.027 \leq A \leq 0.335$m	Increase of 41% in Nu at Re < 8000
1976	Mamayev. et al [5]	Air, fully developed flow in a tube	$540 \leq Re \leq 11000$ $0.5 \leq f \leq 24$ Hz	Up to 44% increase in the heat transfer coefficient at f=12Hz in the turbulent regime

Table 2.1 contd

Date	Investigators	Nature of flow	Operating parameters	Results
1979	Karamercan and Gainer [3]	Heated water	$1000 \leq Re \leq 50000$ $0 \leq f \leq 5$ Hz	Maximum increase in the heat transfer coefficient up to a factor of 5.84
1988	Liao and Wang [4]	Water in heated tube	$3400 \leq Re \leq 27000$ $0.074 \leq f \leq 0.385$Hz	Decrease of 20 % in heat the transfer coefficient without flow reversal and an increase up to 25 % with flow reversal.
1989	Al-Haddad and Al-Binally [16]	Heated air in a tube.	$1000 \leq Re \leq 40000$ $5 \leq f \leq 60$Hz	Increase in Nu above a critical dimensionless number $(Re\,\omega^*)$.
1992	Genin et al. [15]	Water in a heated tube	$10000 \leq Re \leq 25000$ $0.2 \leq f \leq 6$ Hz	No significant effect on Nu
1993	Isshiki et al. [17]	Air in a heated tube	Re =7450. f in the ratio 0.32 to 3.3 of turbulent bursting frequency, f_b	Nu unchanged at $f > f_b$ and varied periodically at $f < f_b$

by superposing an oscillating pressure gradient on the steady driving flow pressure. A slug flow, one dimensional assumption was used to determine the velocity distribution. The solution involved three parameters namely; dimensionless frequency, Prandtl number and amplitude of pressure oscillation. The result showed a sinusoidal axial variation of wall temperature (and hence Nusselt number) along the length of the channel. For high frequency oscillation and dimensionless amplitude of oscillating pressure gradient of magnitude near unity, wall heat transfer was unaffected. The effect of Prandtl number was mainly on the dimensionless length of oscillation cycle ($\pi / M^2 \mathrm{Pr}$) which was very short for large Prandtl number but long for lower Pr.

Another analytical study was carried out by **Faghri et al.** [19] on laminar, fully developed pulsating pipe flow with constant wall heat flux boundary condition. The velocity field was modeled as the sum of mean part and a fluctuating part caused by a periodic pressure gradient with zero average over one period. This causes temperature fluctuation and additional convective term is created in the energy equation. The result shows that at high frequencies, Nusselt number increases in proportion to the pulsation frequency. However at low frequencies, increase in Nu was found to depend on Prandtl number and another dimensionless pulsation parameter proportional to amplitude.

In a similar analytical study carried out by **Siegel** [20], pressure gradient and velocity solution for a slow laminar, fully developed channel flow with uniform heat flux were modeled as the sum of a steady and fluctuating parts. In his solution for the dimensionless steady temperature distribution, the flow oscillation which interacts with the positive temperature gradient along the channel induces axial diffusion of energy which opposes the flow direction. This tends to inhibit the heat transfer process by increasing the wall temperature thereby resulting into a reduction in the overall channel heat transfer coefficient.

Cho and Hyun [21] studied numerically, heat transfer in the laminar, fully developed pulsating pipe flow subjected to a uniform wall temperature boundary condition. Complete time dependent boundary layer equations were solved over a range of oscillation amplitudes and frequency parameters while Pr was set at 7.0 in the computation. Their result showed that in the fully developed region , Nu either increased or decreased depending on frequency parameter while its trend was amplified as amplitude increased. However, for high frequency, the effect of pulsation is confined to the thin layer near the solid wall.

Kim et al. [22] carried out a numerical study on heat transfer in the thermally developing region of a laminar, pulsating channel flow with uniform wall temperature. Here, complete non-steady Navier - Stokes equations were solved to simulate a slow, through flow with Re and Pr maintained at 50 and 0.7 respectively. Flow data were obtained for a wide range of pulsation amplitudes

and frequencies. They found that for large frequencies, effects of pulsation are confined to the narrow zone adjacent to the wall while changes in Nu due to pulsation are pronounced in the entrance region and minor at far downstream locations. These effects are noticeable at low and moderate frequencies and insignificant at large frequencies.

2.3 Momentum Transfer in Pulsating Flows

Ohmi et al. [23] measured the velocity and pressure distribution of pulsating turbulent flow air as well as water in circular pipes using hot wire anemometer and strain gauge type pressure transducer respectively. Reynolds number in both cases was varied between 7740 and 95900 while pulsation frequencies ranged from 0.0432 to 48.0 Hz. The result showed that in the low frequency range, time averaged magnitude of the velocity profile is nearly the same as the steady flow while the phase angle is flat. The oscillating pressures are also found to decrease, nearly linear along the pipe thereby indicating a nearly constant pressure gradient. However at higher frequencies, the velocity profile has a peak and becomes flatter while the phase angle increases near the wall but flat in the central region. Approximate solutions were also derived using a four region model and these solutions agreed very well with the experimental data.

Clamen and Minton [24] carried out an experimental investigation of flow in an oscillating pipe. Flow visualization, using hydrogen bubble technique revealed harmonic velocity pulsations caused by harmonic pressure gradient. The oscillating velocity as well as flow reversal were detected close to the wall.

Genin et al. [15] investigated the effect of pulsation on hydraulic resistance of turbulent flow of water in a stainless steel tube. Their result showed an increase between 10 to 50 % in the coefficient of resistance for Reynolds number in the range 1000 to 25000 and pulsation frequencies between 0.2 Hz and 6.0 Hz.

Carvalho [25] carried out a numerical simulation of behavior of solid inert particles in pulsating flows inside combustors using a computational scheme based on fourth order Runge-Kutta method. The velocities of the particles as a function of time for pulsed and steady flows were compared. The result shows that pulsation decreases the particle residence time in the combustor and increase the rate of particulate emission. This becomes significant as pulsation frequency increases and when the particle diameter is close to the cut diameter that is, the diameter for which the particle starts to rise in the ascending gas flow of the combustor.

2.4 Heat Transfer Enhancement and Pulsation

From the studies reviewed above it is quite evident that pulsation will enhance heat transfer coefficient under certain conditions of the control parameters such as: the frequency, amplitude, wave-form, location of the pulsator and the flow Reynolds number. It is also observed that heat transfer enhancement is more significant for more viscous fluids. The study carried out by **Kastner and Shih** [26] showed that flow pulsation of sufficient frequency and amplitude can highly lower the critical Reynolds number (compared to steady flows) and steepens the velocity profile close to the wall. This is likely to reduce the boundary layer thickness where heat transfer by viscous effect dominates and as a result, an increase in the level of turbulence as well as the heat transfer coefficient is expected. In low frequency pulsating flows, It has been proposed by **Lemlich** [12] and verified as reported in the studies of [3, 4] that appreciable improvement in heat transfer coefficient occurs when pulsation amplitude is large enough as to allow momentary flow reversal during each cycle. However, for flow of high Reynolds number, the effect of turbulent intensity becomes significant. In this case, depending on the frequency of pulsation, either the turbulent intensity or pulsation frequency can be dominant. It is thus expected that the effect of turbulence and pulsation on heat transfer coefficient will depend on both the flow Reynolds number and

frequency of pulsation. Also, [16] reported that for low pressure systems, the amplitude of pulsation has negligible effect on heat transfer coefficient.

2.5 Other Studies on Heat transfer Augmentation

Apart from pulsation there are other methods proposed and verified for increasing the heat transfer in internal flows. Some of these methods are reviewed below:

2.5.1 Abrupt Expansion

Considerable enhancement of the average heat transfer coefficient in the separated flow region beyond an abrupt expansion of flow in a circular channel was reported by **Ede et al.** [27] and **Zemanick and Doughall** [28].

2.5.2 Use of Fins

Habib et al. [29] introduced staggered fins of different spacings into a rectangular duct of turbulent air flow whose Reynolds number ranged between 8000 and 18000. Their results showed significant enhancement of heat transfer due to flow deflection and impingement upon the fins. Increase in Reynolds number, thermal conductivity of fins and decrease in fin spacing and wall heat flux, all contributed to the enhancement obtained.

Edwards et al. [30] studied the local heat transfer characteristics in the entrance region of turbulent air flow in an annuli with inner cylinders fitted

with longitudinal fins. Reynolds number was varied between 4000 and 15000 Considerable enhancement of the heat transfer coefficient was recorded. The enhancement ratio depends on Reynolds number and fin spacing.

2.5.3 Turbulent Promoters

Habib and McElligot [31] recorded appreciable increase in heat transfer coefficient when swirl was introduced at the inlet of an abrupt pipe expansion.

Nakatani and Suzuki [32] carried out flow visualization and heat transfer measurements for flow between parallel plates with an insertion of staggered array of cylinders at Re = 8500. Heat transfer was found to be enhanced due to the effect of intermittent reattachment of discrete vortices formed in the separation shear layer close to the cylinder surfaces.

Increase in heat transfer coefficient by a factor up to 2.27 was also reported by **Prasad and Brown** [33] due to insertion of wire - coil springs at the inner surface of a horizontal inner tube of a double pipe heat exchanger undergoing turbulent flow. The Reynolds number ranged from 40000 to 97000.

2.6 Models of Pulsating Turbulent Flows

Hydrodynamics and thermal behavior of pulsating flows and hence the phenomenon of enhancement or reduction of heat transfer coefficient has

attracted the use of some models of turbulence in predicting results as well as making sense out of available experimental data. Two of these models are discussed here, namely: model of quasi-steady flow and model of turbulent bursting (viscous sublayer renewal).

2.6.1 Quasi - Steady Flow Model

In this model, it is assumed principally that pulsating frequencies are very low such that the usual steady state correlation for heat transfer coefficient or Nusselt number holds at every instant. This means that the velocity and temperature profiles can be replotted and at any point in time, correspond to the value of the Reynolds number at that moment. A general illustration of this model as carried out by **Lemlich** [12] is given below:

For a forced convection in which the mass flow rate of a fluid with constant physical properties is undergoing periodic variation, by conservation of mass, the time averaged velocity over a cycle period of $1/f$ can be obtained by

$$V_m = f\int_0^{1/f} V d\tau \qquad \textbf{(2.2)}$$

and the heat transfer coefficient can be approximated within a reasonable limit of the mass flow rate as:

$h = kV^n$ for flow with pulsation and **(2.3a)**

$h' = kV_m^n$ for corresponding flow without pulsation **(2.3b)**

where n is a constant

The time averaged heat transfer coefficient for pulsation is given by:

$$h_m = f\int_0^{1/f} h d\tau \tag{2.4}$$

For a small change in temperature difference, ΔT throughout the cycle, energy balance over a cycle period gives the total heat transferred as:

$$Q = \frac{h_m A_r \Delta T}{f} = A_r \Delta T \int_0^{1/f} h d\tau \tag{2. 5}$$

where A_r is the heat transfer area.

Dividing Eqn.(2.4) by Eqn.(2.3b) and using Eqn.(2.2) and Eqn.(2.3a), we have:

$$\frac{h_m}{h'} = \frac{f\int_0^{1/f} kV^n d\tau}{k(f\int_0^{1/f} V d\tau)^n} = \frac{f^{1-n}\int_0^{1/f} V^n d\tau}{(\int_0^{1/f} V d\tau)^n} \tag{2.6}$$

Let $\theta = 2\pi f$, then

$$d\theta = 2\pi f d\tau \tag{2.7}$$

Substituting Eqn. (2.7) into Eqn.(2.6), we finally obtain the heat transfer ratio known as improvement ratio [14], given as:

$$\frac{h_m}{h'} = \frac{(2\pi)^{n-1}\int_0^{2\pi} V^n d\theta}{(\int_0^{2\pi} V d\theta)^n} \tag{2.8}$$

For any wave form of pulsation, Eqn.(2.8) is independent of frequency. Also for $n < 1$, it predicts a relative decrease in Nusselt number while an increase is predicted for $n > 1$ and no change for $n = 1$. Even though in this model relative heat transfer coefficient is independent of pulsation frequency, there are certain

frequency levels above which the system is no longer quasi-steady and the prediction fails, although this has not been fully established [12].

For sinusoidal pulsation of amplitude A and circular frequency ω, flow velocity becomes :

$$V = V_s + \frac{d}{dt}(ASin\omega t) = V_s(1 + BCos\omega t) \tag{2.9}$$

where V_s is the steady component of the velocity and

$B = \frac{\omega A}{V_s}$, is known as relative velocity oscillation amplitude.

By substituting Eqn.(2.9) into Eqn. (2.8), the improvement ratio becomes:

$$\frac{h_m}{h'} = \frac{1}{2\pi}\int_0^{2\pi}(1 + BCos\theta)^n d\theta \tag{2.10}$$

Thus, according to quasi - steady model, improvement ratio for sinusoidal pulsations, as can be seen from Eqn.(2.10) depends only on relative pulsation amplitude, B. In the case where $B > 1$, reverse flow occurs in the duct and this results in increase in relative heat transfer coefficient while for $B < 1$, there is no flow reversal and Eqn. (2.10) predicts a reduction in the relative heat transfer coefficient. Such effect was observed in the study carried out by **Liao and Wang** [4].

2.6.2 Turbulent Bursting Model

Turbulent bursts are series of quasi-cyclic or periodic activities that occur near the wall of turbulent boundary layer and has been related to the well known phenomenon of intermittence in the small scale structure of turbulence. This intermittent occurrence of bursts at the edge of the inner layer plays a key role in turbulent energy production [34]. A more conceptual way of explaining this model according to **Genin et al.** [15] is that the viscous sublayer is unstable, that is, it grows and collapses in a periodic manner in the statistical sense of the process. Its thickness increases to a certain critical level but the layer of retarded fluid very close to the wall looses stability and breaks down (bursts), thereby releasing mass into the core of the flow and simultaneously, a new sublayer is formed or 'renewed'. These bursts according to studies carried out by **Mizushina et al.** [35] take place at certain 'preferred' range of frequencies centered around a mean frequency. They obtained the upper and lower limit of this range from a histogram of frequency of occurrence of bursts and these frequencies are found to be dependent on flow Reynolds number in the range $10^3 - 10^5$. From their measurements, **Ramaprian and Tu** [36] developed approximate relationships for the mean, upper and lower bound of this range which are expressed respectively below as:

$$\omega D / U^* \approx 1.58\, Re^{0.125} \tag{2.11}$$

$$\omega_{bU} D / U^* \approx 31\, Re^{0.125} [10^{-(3.32-0.667 \log Re)} \tag{2.12}$$

$$\omega_{bL} D / U^* \approx 166\, Re^{-0.54} \tag{2.13}$$

where $D =$ pipe diameter

$\omega = 2\pi f_b$, is the circular bursting frequency and

$U^* = (\tau_0 / \rho)^{1/2}$, is the friction velocity.

2.6.2.1 Effect of Pulsation on Turbulent Bursting Frequencies

There is no doubt that besides the fact that pulsation varies the mass flow rate about its mean value, it may also affect the turbulent exchange process. It has been discussed in the literature [4, 15, 36] that this phenomenon is related to the bursting process in the turbulent boundary layer. **Mizushina et al.** [34] found that if the pulsation frequency is close to the turbulent burst frequency, then certain resonance interaction occurs which may show up as stimulation or suppression of corresponding frequencies in the turbulent energy spectrum and as changes in the characteristics of turbulent transfer. Consequently, this has its effect on the increase or reduction of heat transfer coefficient . However, when pulsation frequency lies outside the preferred range, such pulsation does not affect turbulent burst and the mean bursting frequency is equal to that of steady flow at the same Reynolds number.

In order to relate the pulsation frequency to the turbulent bursting frequencies, the pulsation frequency is non-dimensionalised in the form of the dimensionless bursting frequencies which will now be a function of Re. This will be compared with the relations given in Eqns. (2.11), (2.12) and (2.13) respectively at different Reynolds numbers. In doing this, U^* is calculated from the coefficient of resistance, λ, defined by Blasius formula [37] given as:

$$\lambda = 0.3164\,\mathrm{Re}^{-0.25} \tag{2.14}$$

The friction velocity can be expressed as:

$$U^* = (\tau_0/\rho)^{1/2} = (1/8\,\lambda\overline{U}^2)^{1/2} \tag{2.15}$$

Substituting Eqn. (2.14) into Eqn. (2.15), we get:

$$U^* = \frac{0.1988718\overline{U}}{Re^{0.125}} \tag{2.16}$$

Hence we obtain:

$$\omega D / U^* = \frac{2\pi f D\, Re^{0.125}}{0.1988718\overline{U}} \tag{2.17}$$

where $\overline{U}$ = flow average velocity,

and f = frequency of pulsation

The term $\omega D / U^*$ is a dimensionless frequency described as the equivalent turbulent stokes number which can be used to characterize periodic turbulent

flow. This is a measure of the relative distance from the wall up to which the unsteady effects in the flow will penetrate [36].

Ramaprian and Tu [36] classified pulsating flows into several regimes as shown in Fig. 2.1. Regime A which lies below the lower bound of the bursting frequency line is the 'low frequency zone' and the bursting frequency is not a function of pulsation frequency. Where $\omega D / U^*$ is much less than ω_{bL} / U^*, the turbulent structure becomes quasi-steady and the heat transfer coefficient is expected to decrease with pulsation and behave in a manner of the quasi-steady model. In other words, pulsation frequency is not expected to have any effect on heat transfer.

Regimes B and C cover the preferred range of the bursting frequency. Regime B is called the 'intermediate frequency regime' and the mean bursting frequency is suppressed due to resonance occurring at pulsation frequency. Heat transfer behavior is therefore expected to be affected. In regime C, the imposed pulsation frequency will interact strongly with the turbulent bursting process at the wall. In this preferred range, Nusselt number is expected to increase with pulsation.

Regime D is called the rapid oscillation or region of fast pulses where there is a very strong interaction between imposed pulsation and turbulence structure. However, the effect of pulsation on turbulence structure as well as heat transfer has not attracted adequate studies in this regime [4 , 15, 36]

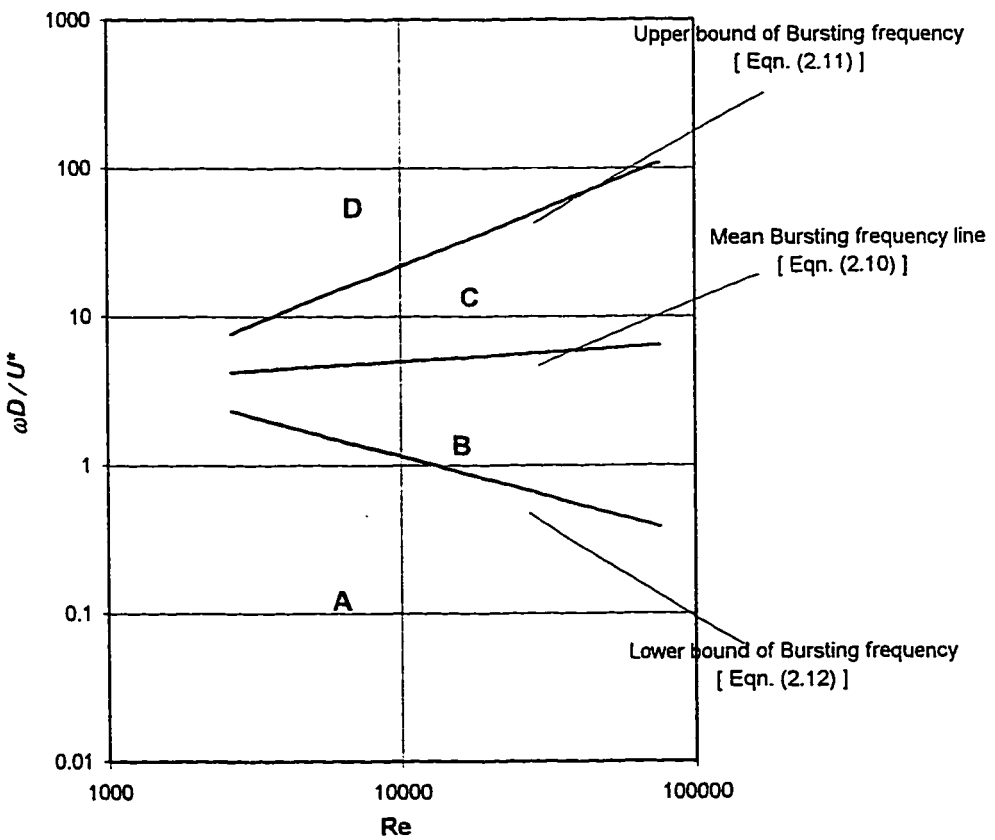

Fig. 2.1 Classification of unsteady (periodic) turbulent flows

CHAPTER 3

EXPERIMENTAL SET-UP

This chapter presents the detailed description of the test rig which includes: the air supply unit, test section, pulsating mechanism and instrumentation.

3.1 The Test Rig

The test rig is an open loop system in which air, as the working fluid is admitted near atmospheric pressure by a blower and is discharged to the atmosphere through the test section after being heated. The schematic diagram of the test set-up is as shown in Fig. 3.1

3.1.1 Air Supply Unit

This unit consists of the air blower, piping system, orifice meter, settling chamber and the calming section. The electric air blower, made of cast iron runs at a constant speed of 3000 r.p.m. It has a 0.15 m (6 inch) diameter outlet port which is connected to the PVC piping system of the same nominal diameter. A constant mass flow rate is maintained and controlled by metering the air through the main and by-pass valves, respectively. The flow rate was measured

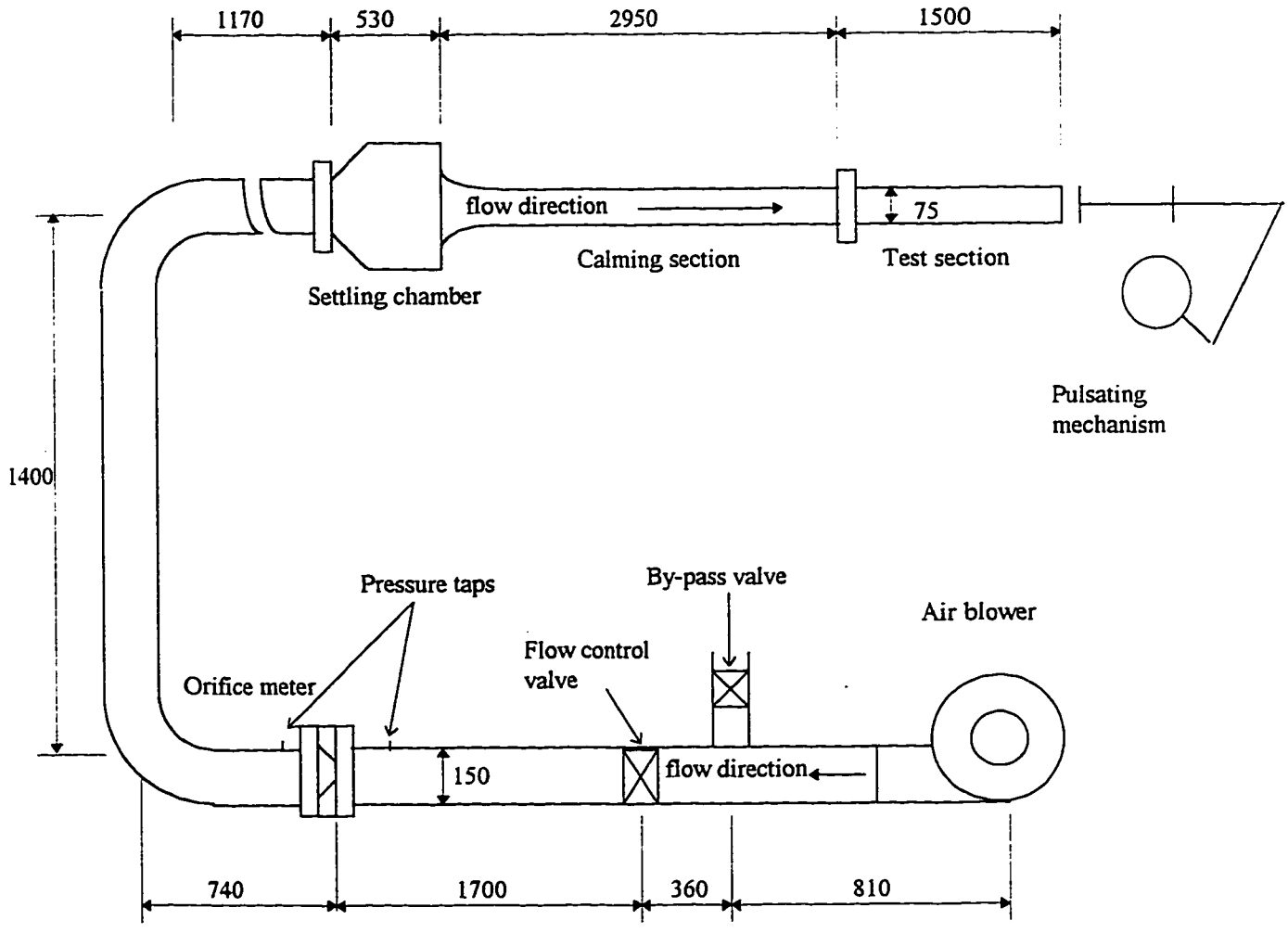

(Dimensions are in mm)

Fig. 3.1 Test Set-up.

through pressure drop across a calibrated sharp-edged orifice installed between two flanges at approximately 2.87 m. from the blower. The upstream and downstream pressure taps are located: respectively, at 0.16 m. and 0.11m. from the orifice. This is equivalent to 1.067 and 0.73 flow line diameters and therefore corresponds to the vena contracta tap connection as recommended by **Stearns et al.** [38]. The air is admitted in a 0.3 m. diameter and 0.53 m average length settling chamber, made of mild steel. This serves the purpose of damping flow instabilities before velocity development takes place in the calming section. The calming section is a 0.075 m. internal diameter copper pipe preceding the test section. Its length is at about 40 pipe diameters long so that the flow becomes hydrodynamically fully developed before heating takes place at the test section.

3.1.2 Test Section

The test section, shown schematically in Fig. 3.2 is a copper pipe of 1.5 m length (L), 0.075 m. internal diameter (D) and 0.0025 m. thickness (t). It is connected to the calming section through two flanges. The pipe wall temperatures are measured directly by 10 K- type thermocouples whose junctions are embedded inside holes each of diameter 0.002 m and depth 0.0015 m. drilled into the pipe surface. The position of the tenth thermocouple corresponds to the effective length of the test section (L_e), which is 1.025 m. and is equivalent to 13.6 pipe diameters. The air inlet temperature is determined from another K- type thermocouple, enclosed in a ceramic tube which is

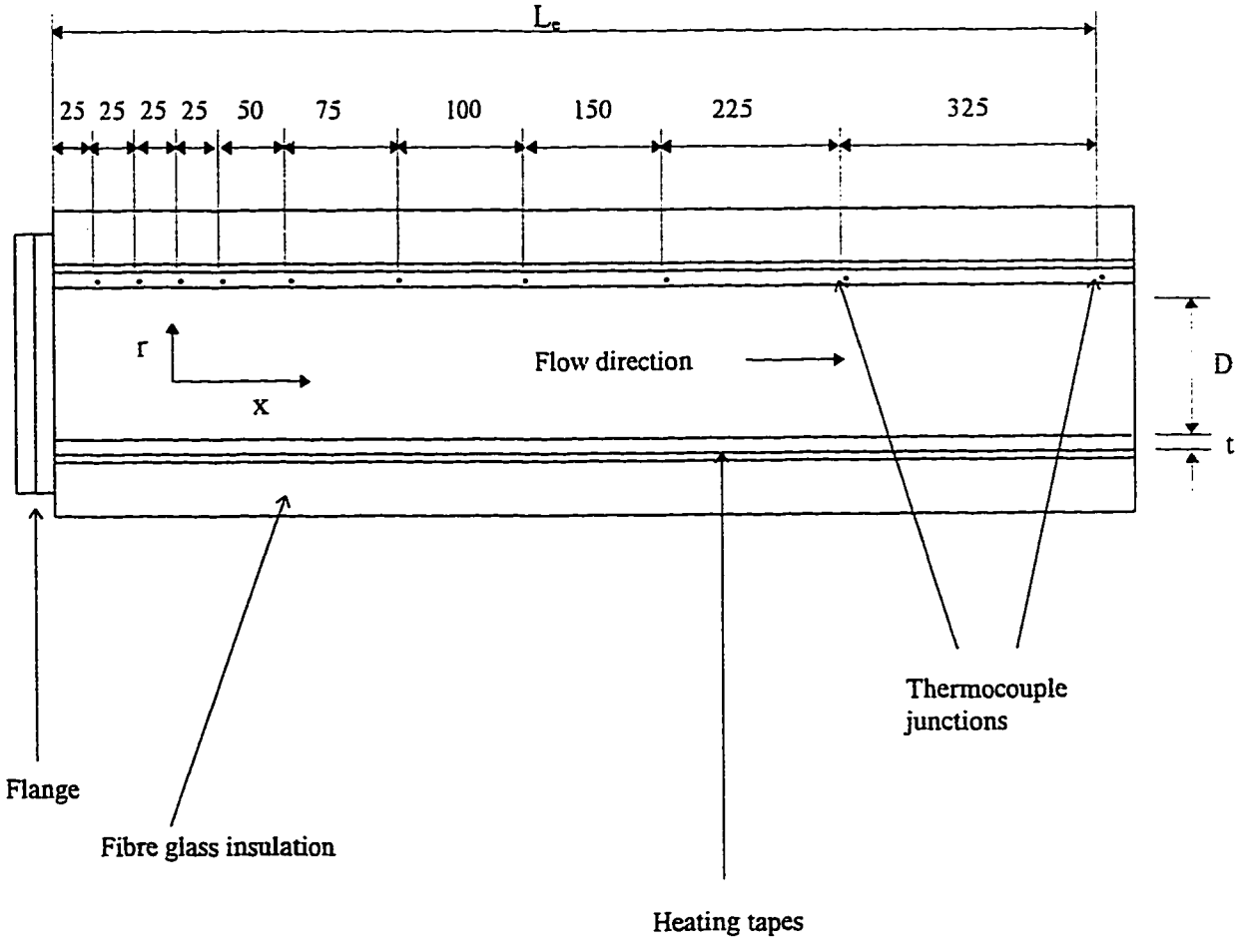

(Dimensions are in mm.)

Fig. 3.2 Test section

inserted in a hole drilled through the flanges at the inlet. The flanges are insulated from each other in order to avoid 'backward' axial conduction to the calming section. Heat is supplied to the pipe wall through six Amox fiber insulated heating tapes, each of length 2.438 m (8 ft.) and 0.025 m. width. The tapes are of equal wound length of approximately 0.236 m. along the pipe. The test section together with the wound tapes are insulated by fiber glass insulation material in form of an annulus of approximately 0.08225 m. and 0.1426 m. internal and external diameters respectively.

3.1.3 Pulsating Mechanism

The pulsating mechanism is located downstream the test section at the pipe exit. It is a four bar slider crank mechanism, driven by a variable voltage D.C. motor. As shown in Fig. 3.3, the slider (link 4) is connected to a flexible disc piston which opens and closes the pipe as it oscillates back and forth, thereby inducing the flow pulsation. The displacement amplitude is equivalent to the stroke of the piston which can be adjusted by altering the pivot point along link 3 which is connected to the slider. However, this amplitude is kept constant throughout the experiment by fixing this point of pivot. The frequency of the oscillating piston (hence pulsation frequency) corresponds to the rotational speed of the motor.

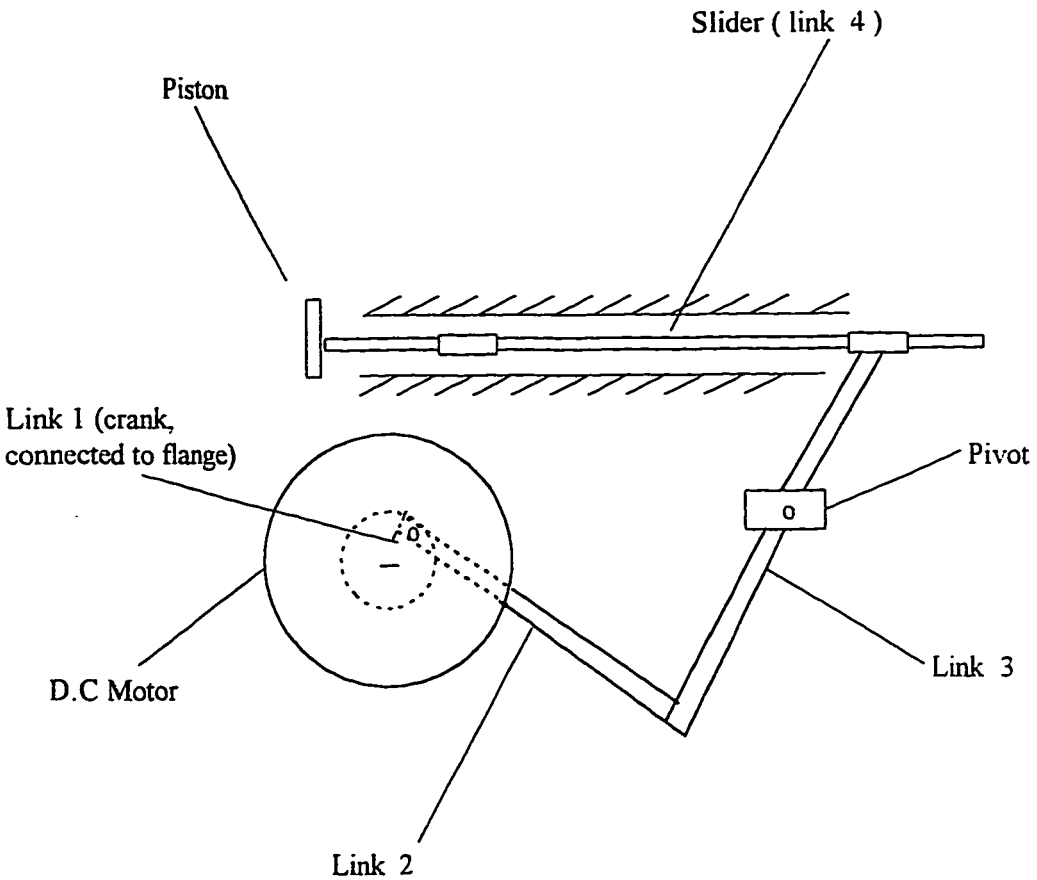

a. Schematic diagram of the pulsating mechanism

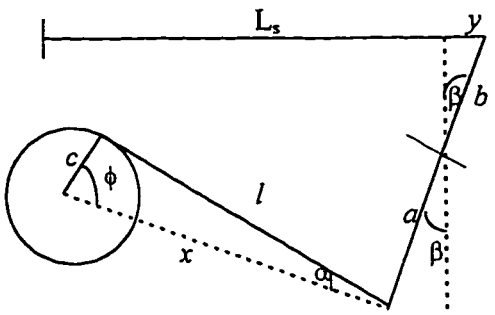

b: Kinematic analysis of the pulsating mechanism

Fig. 3.3 Pulsating mechanism.

3.1.3.1 Kinematic Analysis of the Pulsating Mechanism

From Fig. 3.3b , the displacement, x between the crank and link 2 gives rise to angular displacement of link 3 about the pivot which in turn results into the displacement of the slider L_s, (link 4) whose motion is constrained in the horizontal direction as shown. Hence, from the diagram:

$$x = cCos\phi + lCos\alpha \tag{3.1}$$

Using Sine formula, we have:

$$Sin\alpha = \frac{c}{l}Sin\phi \tag{3.2}$$

Expressing $Cos\alpha$ in terms of ϕ , we get:

$$Cos\alpha = \left[1 - \left(\frac{c}{l}\right)^2 Sin^2\phi\right]^{1/2} \tag{3.3}$$

Substituting the above into Eqn. (3.1), we have:

$$x = cCos\phi + l\left[1 - \left(\frac{c}{l}\right)^2 Sin^2\phi\right]^{1/2} \tag{3.4}$$

$$dx = -cSin\phi\left\{1 + \frac{c}{l}Cos\phi\left[1 - \left(\frac{c}{l}\right)^2 Sin^2\phi\right]^{-1/2}\right\}d\phi \tag{3.5}$$

For small angle $d\beta$, we can write:

$$dx = ad\beta$$

Thus, $$d\beta = \frac{dx}{a} \tag{3.6}$$

The differential displacement, dy of the slider can be approximated by a differential arc length subtending β and adjacent to b hence,

$$dy = bd\beta = -\frac{bc}{a} Sin\phi \left\{ 1 + \frac{c}{l} Cos\phi \left[1 - \left(\frac{c}{l}\right)^2 Sin^2\phi \right]^{-1/2} \right\} d\phi \qquad \textbf{(3.7)}$$

Integration of Eqn. (3.7) between the limit $\phi = 0$ to any arbitrary value of ϕ yields the displacement of the slider induced pulsation given by:

$$y = \frac{b}{a} \left\{ cCos\phi + l \left[1 - \left(\frac{c}{l}\right)^2 Sin^2\phi \right]^{1/2} \right\} - \frac{b}{a}(c + l) \qquad \textbf{(3.8)}$$

Replacing ϕ by $\omega t = 2\pi f t$, where ω is the angular velocity of the motor which corresponds to the circular frequency of pulsation, Eqn. (3.8) can be written as:

$$y = \frac{b}{a} \left\{ cCos(\omega t) + l \left[1 - \left(\frac{c}{l}\right)^2 Sin^2(\omega t) \right]^{1/2} \right\} - \frac{b}{a}(c + l) \qquad \textbf{(3.9)}$$

Differentiation of Eqn. (3.9) with respect to time yields the velocity of the piston which induces pulsation to the flow. Hence, differentiating Eqn. (3.9) yields:

$$\frac{dy}{dt} = V_P = -\frac{bc}{a} Sin(\omega t) \left\{ 1 + \frac{c}{l} Cos(\omega t) \left[1 - \left(\frac{c}{l}\right)^2 Sin^2(\omega t) \right]^{-1/2} \right\} \omega \qquad \textbf{(3.10)}$$

Direct measurement of the links of the mechanism at the desired adjustment of the pivot (which controls the value of a and b) yields the following values:

$c = 0.026$ m., $l = 0.205$ m., $a = 0.143$ m. and $b = 0.063$ m.

Substituting the above values into Eqn. (3.10) , the pulsation inducing velocity of the piston as a function of time for different frequencies can be obtained as shown in Fig. 3.4. The amplitude of the oscillating velocity, as can be seen is proportional to the pulsation frequency. A comparison between the piston velocity and a pure sinusoidal wave shows clearly an almost sinusoidal trend as shown in Fig. 3.5.

3.2 Instrumentation

In order to obtain as accurate and reliable data as possible, the following instruments were used in the experiment:

3.2.1 Manometer

Betz type projection micro-manometer was used to determine the pressure drop across the orifice meter. The instrument with resolution of 0.2 mm uses water as the manometer fluid.

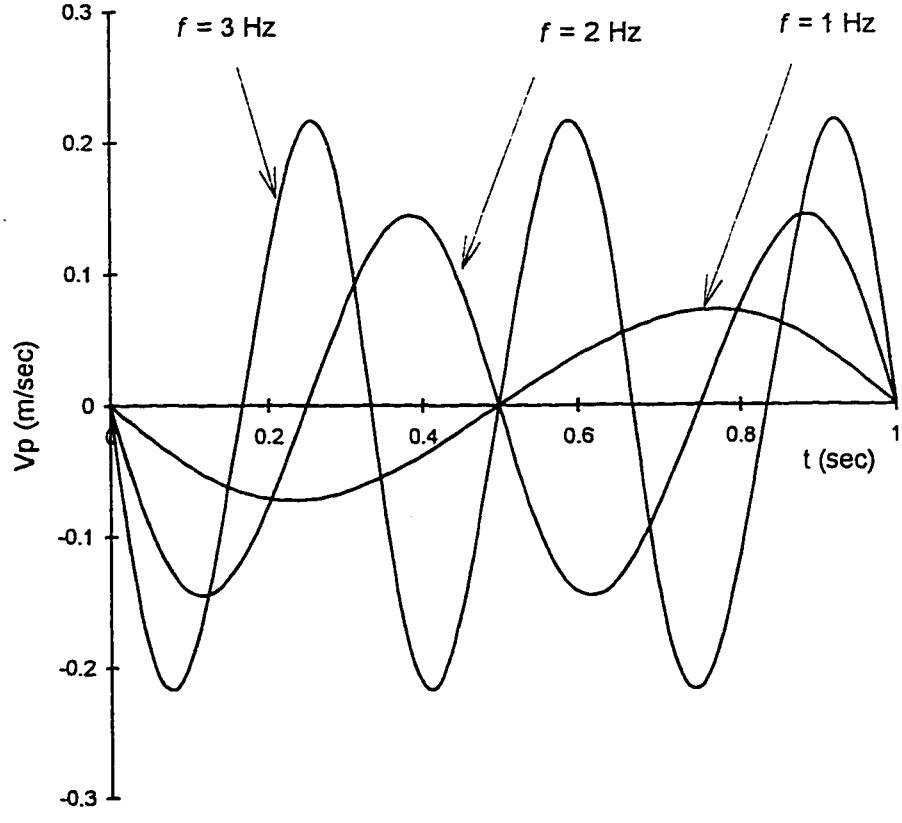

Fig. 3.4 Nearly sinusoidal velocity of the oscillation inducing piston as a function of time at different frequencies

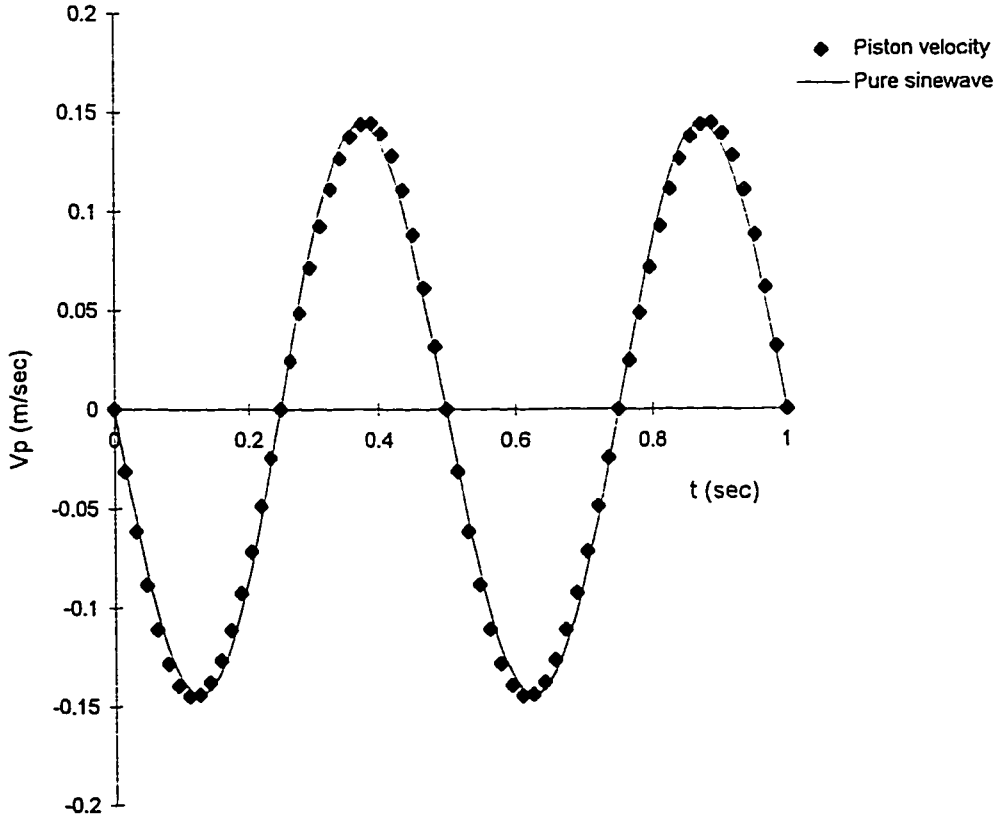

Fig. 3.5 Comparison between oscillating piston velocity and a pure sinusoidal wave form (f = 2Hz)

3.2.2 Heaters and Power meters

Heating power was supplied using six variable voltage transformers, five of which are of 220 volts input, made by Lab Sciences and one Voltac, model TSB-5 of 110 volts input. They were employed in providing uniform heat flux to the wall of the test section. The supplied power was measured using Clarke-Hess, model 259 digital V-A-W meter.

3.2.3 Thermometers

The surface temperatures were measured using Omega, model 2176A multipoint digital thermometer. The instrument can operate with thermocouple types J, K, T ,E and of $0.2^{o}C$ resolution. The fluid inlet temperature was measured with Omega, model 871 digital thermometer of $0.1^{o}C$ resolution.

3.2.4 Tachometer

The angular velocity of the D.C. motor which is equivalent to the pulsating frequency was measured by using Cole-Parmer, model 8200-50 digital tachometer with a photo electric probe.

CHAPTER 4

EXPERIMENTAL TECHNIQUES

4.1 Introduction

This chapter presents calculations for all relevant parameters showing how raw data are reduced to the desired values of heat transfer coefficients and Nusselt numbers, for both steady and pulsed flows. The procedure for running the experiment is also described and finally, uncertainty analysis for measured and calculated parameters are carried out in order to examine the accuracy of the results.

4.2 Test Procedure

Before the test run commenced, the flow line was properly aligned and as the blower was switched on, the whole system was checked against any air leakage. The flow control and by-pass valves were adjusted until the desired manometer reading (hence the desired flow Reynolds number at the test section) was achieved. As expected from the analysis carried out in section 3.1.3.1, the pulsed flow was characterized by almost a sinusoidal oscillation of the manometer fluid level and this was set to oscillate about the required level of

the corresponding steady flow. The room temperature was recorded and conditioned against arbitrary variation. As regards to the relative settings of flow and power during the test series, it was felt that coherent mass of data could be collected if the heat flux is adjusted in proportion to the mass flow rate so as to give a fairly uniform rise in the bulk mean temperatures. In order to validate the assumption of constant fluid properties along the test section and at the same time have a considerable bulk-to-surface temperature difference, axial temperature rise between 10 ^{o}C and 15 ^{o}C was maintained.

Depending on the flow rate and power settings, considerable length of time was required to achieve steady state conditions for pulsed flow and corresponding flow without pulsation. This was observed to be longer for low flow rates and shorter for higher flow rates. Data was collected when the pipe surface temperatures showed virtually no variation or variation of less than 0.2 ^{o}C per hour. The data was fed into a data reduction computer program (sample programs and output are shown in the appendix) through which the values of the Reynolds numbers, local and average heat transfer coefficients and Nusselt numbers for both steady and pulsed flows are calculated.

4.3 Data Collection

The measured parameters include: the air mass flow rates, power supplied and heat loss, surface temperatures of the pipe along the test section,

fluid inlet temperature and the frequencies of pulsation. Using these data, the fluid bulk mean temperatures, heat transfer coefficients and Nusselt numbers were determined.

4.3.1 Mass Flow Rates

The mass flow rate is determined from the pressure drop across the orifice meter using the following relation [39]

$$\dot{m} = C_d \rho . A_o \left[2g\left(\frac{\rho_l}{\rho} - 1 \right) \Delta h \right]^{1/2} \tag{4.1}$$

The discharge coefficients for different Reynolds numbers were calculated based on empirical relations described by **Stearns et al.**[38] which takes into account all necessary design parameters for orifice meters. For 0.5 and 0.4 orifice to the main flow line diameter ratio (with vena contracta pressure tap connections), the relations for the discharge coefficients C_d are determined by [38]:

$$C_{d(0.5)} = 0.6247\left(1 + \frac{539.8902}{\mathrm{Re}}\right) \tag{4.2a}$$

$$C_{d(0.4)} = 0.6085\left(1 + \frac{280.7998}{\mathrm{Re}}\right) \tag{4.2b}$$

In order to ensure accurate determination of the mass flow rates through the the calculated discharge coefficients for the orifice-plate meters, a calibrated

rotameter was connected to the flow line. The rotameter readings were in excellent agreement with the calculated flow rate values obtained using the pressure drop across the orifice at the same manometer readings as shown in Fig. 4.1

As a further check, the mass flow rate was also determined from the mean velocity calculated by integrating the velocity profile measured with a Pitot-static tube, downstream the test section at the fully developed region for the case of Reynolds number of 14867 (Fig. 4.2). The result is in very good agreement with the corresponding value from the orifice meter.

4.3.2 Heat Input

To obtain the heat input to the test section through the heating tape segments, input currents, voltages and power were measured simultaneously. The digital wattmeter which provides a direct readout of the power was used to measure the power input. The voltage was adjusted to achieve uniform input power (hence uniform heat fluxes) at the pipe wall.

4.3.3 Pipe Surface Temperatures

The pipe surface temperatures as well as fluid inlet temperatures for both steady and pulsed flow were measured directly using the K-type thermocouples and readout from the digital read-out devices.

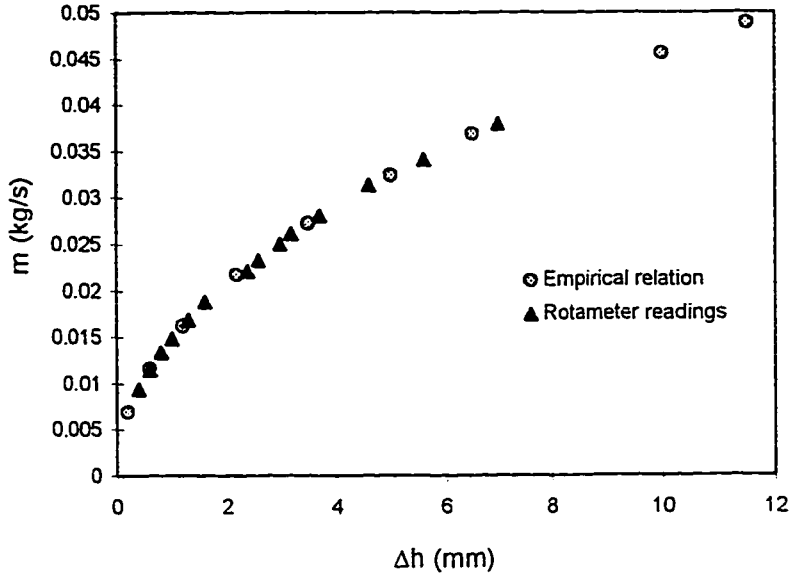

Fig. 4.1 Orifice meter calibration curve.

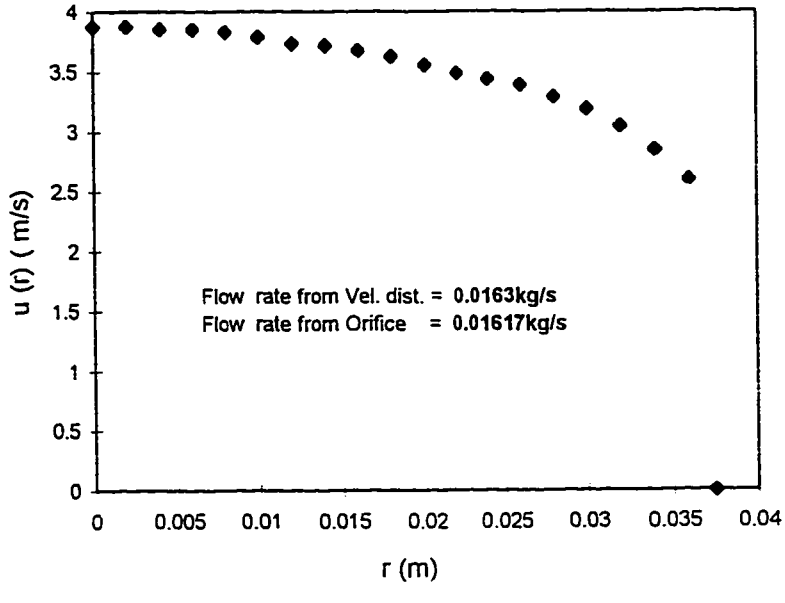

Fig. 4.2 Velocity distribution across the pipe **(Re = 14867)**

4.3.4 Heat Loss

Heat loss was assumed to be through the insulation only. To determine the heat loss, the outer surface temperatures of the insulation were measured at the corresponding points where the pipe surface temperatures were obtained. Using the Fourier law of radial heat conduction, based on cylindrical model with inside radius of 0.0822 m. and outside radius of 0.142 m., the heat flux through the insulation at the center of each heater segment was determined and given as:

$$\dot{q}_{loss} = -k \frac{[T_{cso}(x) - T_{cs}(x)]}{R_{cs} \ln(R_{cso}/R_{cs})} \tag{4.3}$$

The corresponding heat transferred into the fluid was calculated by subtracting the heat loss at each heater segment from the heat input. This heat loss analysis was carried out for steady flow and the heat transferred from each segment was found to be constant within difference of 1.4 %. Similar results were obtained for pulsed flow. The total heat loss from the heaters was therefore calculated to be 6.2 % of the total heat input.

4.3.5 Fluid Local Bulk Mean Temperatures

The local bulk mean temperatures of the fluid at the end of each heater segment was determined using energy balance as follows:

$$T_{j,o} = \frac{q_j}{\dot{m} C_p} + T_{j,i} \tag{4.4}$$

where q_j = Heat transferred to the fluid at jth segment.

$T_{j,i}$ = Fluid inlet temperature to the jth segment.

$T_{j,o}$ = Fluid outlet temperature at the jth segment.

The local bulk mean temperatures at the corresponding points along the test section where the pipe wall temperatures are measured are determined by linear interpolation of the mean temperatures at the end of the heater segments.

4.3.6 Pulsation Frequency

The frequency of pulsation corresponds directly to the rotational speed of the D.C motor whose output shaft is connected to a flange that drives the crank of the pulsating mechanism. This is determined by employing a digital tachometer with a photo electric probe. This probe emits light unto the flange of the motor which is taped at one side with a reflector. As the flange rotates, each reflection is counted by the probe. The number of reflections per minute is a measure of the speed of the motor hence, the frequency of pulsation.

4.4 Data Reduction

The data obtained by measurements and calculations were reduced to obtain the flow Reynolds numbers, heat transfer coefficients and Nusselt numbers as described below:

4.4.1 Reynolds Number

The flow Reynolds number at the test section is determined by:

$$\mathrm{Re} = \frac{4\dot{m}}{\pi D \mu} \tag{4.7}$$

4.4.2 Heat Transfer Coefficient

The total heat flux is obtained by adding up all the heat transferred into each heater segment. This is then divided by the total heat transfer area, hence;

$$\dot{q}_o = \frac{Q_{trans}}{\pi D L} \tag{4.8}$$

The local and average heat transfer coefficients are determined respectively by:

$$h(x) = \frac{\dot{q}_o}{T_s(x) - T_m(x)} \tag{4.9}$$

$$h_{mean} = \frac{1}{L}\int_0^L h(x)dx \tag{4.10}$$

Since the values of local heat transfer coefficient are discrete, the above integration is carried out numerically using trapezoidal rule.

4.4.3 Nusselt Number

Using Eqns. (4.9) and (4.10), the local and mean Nusselt numbers are obtained by;

$$Nu(x) = \frac{h(x)D}{k} \tag{4.11}$$

$$Nu_{mean} = \frac{h_{mean}D}{k} \tag{4.12}$$

4.5 Uncertainty Analysis

In order to estimate the accuracy of the data obtained, uncertainty analysis of various measured parameters are carried out. These analyses are based on the method of **Kline and McClintock** as presented in [40]. It requires specification of uncertainties in the various primary experimental measurements. This can be obtained if the accuracy of such calibrated instrument for the direct measurement is specified by the manufacturer or the uncertainty in such measurement is reasonably and justifiably assigned by the experimenter. These measurements are then used to calculate some desired result of the experiment. For example, if the result R is given as a function of the independent variables

$x_1, x_2, x_3 \ldots\ldots\ldots\ldots\ldots\ldots\ldots, x_n$, then,

$$R = R(x_1, x_2, x_3, \ldots\ldots\ldots\ldots x_n) \tag{4.13}$$

Let w_R be the uncertainty in the results and $w_1, w_2, w_3 \ldots\ldots\ldots\ldots, w_n$ be the uncertainties in the independent variables. The uncertainty in the result is given by

$$w_R = \left[\left(\frac{\partial R}{\partial x_1} w_1\right)^2 + \left(\frac{\partial R}{\partial x_2} w_2\right)^2 + \ldots\ldots\ldots + \left(\frac{\partial R}{\partial x_n} w_n\right)^2\right]^{1/2} \tag{4.14}$$

4.5.1 Uncertainty in the Mass Flow Rate

The primary quantities measured for calculating the mass flow rate are: the area of the orifice meter, A_o and the manometer reading, Δh. Comparing the calculated discharge coefficient for the same diameter ratio, Reynolds number and pressure tap connection with ASME data on fluid meter report given by **Stearns et al.** [38], uncertainty in C_d is estimated to be about 0.8653 %. The orifice meter is machined to very high precision and as a result, uncertainty in the diameter (hence in the area) is considered negligible. The uncertainty in reading the liquid level of the projection micro-manometer used in obtaining the pressure drop across the orifice meter, has been estimated to be 0.05 mm. The uncertainty in the mass flow rate is therefore calculated as follows:

$$\dot{m} = C_d \rho A_o \left[2g\left(\frac{\rho_l}{\rho} - 1\right)\Delta h\right]^{1/2} \tag{4.15a}$$

Differentiating Eqn. (4.15a), we get:

$$\frac{\partial \dot{m}}{\partial C_d} = \rho . A_o \left[2g(\frac{\rho_l}{\rho} - 1)\Delta h \right]^{1/2} = \frac{\dot{m}}{C_d} \tag{4.15b}$$

$$\frac{\partial \dot{m}}{\partial \Delta h} = C_d \rho . A_o \left[2g(\frac{\rho_l}{\rho} - 1) \right]^{1/2} \frac{1}{2\sqrt{\Delta h}} = \frac{\dot{m}}{2\Delta h} \tag{4.16}$$

$$w_{\dot{m}} = \left[\left(\frac{\dot{m}}{C_d} w_{Cd} \right)^2 + \left(\frac{\dot{m}}{2\Delta h} w_{\Delta h} \right)^2 \right]^{1/2} \tag{4.17}$$

where $w_{\dot{m}}$, w_{Cd}, and $w_{\Delta h}$ are the uncertainties in the mass flow rate, discharge coefficient and manometer reading respectively.

Dividing both sides of Eqn. (4.17) by $\dot{m}$, we have:

$$\frac{w_{\dot{m}}}{\dot{m}} = \left[\left(\frac{w_{Cd}}{C_d} \right)^2 + \left(\frac{w_{\Delta h}}{2\Delta h} \right)^2 \right]^{1/2} \tag{4.18}$$

For the minimum manometer reading (corresponding to Re = 6387) we have:

$$\Delta h = 0.6mm = 0.6 \times 10^{-3} m$$

$$w_{\Delta h} = 0.05$$

$$\frac{w_{Cd}}{C_d} = 0.8653.\% = 0.008653$$

Substituting these into Eqn. (4.18), the relative uncertainty in the mass flow rate is given as:

$$\frac{w_{\dot{m}}}{\dot{m}} = \left[(0.008653)^2 + (0.0416667)^2\right]^{1/2} = 0.042556$$

$$= 4.256\ \% \qquad \textbf{(4.19a)}$$

Similarly for the maximum manometer reading ($\Delta h = 10mm = 10.0 \times 10^{-3} m$) which corresponds to Re = 41947, the relative uncertainty in the mass flow rate in this case is given as:

$$\frac{w_{\dot{m}}}{\dot{m}} = \left[(0.008653)^2 + (0.0025)^2\right]^{1/2} = 0.009 = 0.9\ \% \qquad \textbf{(4.19b)}$$

4.5.2 Uncertainty in Heat Input, Q

By differentiating the relation, $Q = V.I$, we obtain:

$$\frac{\partial Q}{\partial V} = I \qquad \textbf{(4.20a)}$$

$$\frac{\partial Q}{\partial I} = V \qquad \textbf{(4.20b)}$$

Hence, the uncertainty in the heat input becomes:

$$w_Q = \left[\left(\frac{\partial Q}{\partial V} w_V\right)^2 + \left(\frac{\partial Q}{\partial I} w_I\right)^2\right]^{1/2}$$

$$= \left[(I w_V)^2 + (V w_I)^2\right]^{1/2} \qquad \textbf{(4.21)}$$

Dividing both sides of Eqn. (4.21) by $Q = V.I$, the relative uncertainty in the heat input becomes:

$$\frac{w_Q}{Q} = \left[\left(\frac{w_V}{V}\right)^2 + \left(\frac{w_I}{I}\right)^2\right]^{1/2} \tag{4.22}$$

The relative uncertainty in the measured voltages and currents were each estimated to be about 1 %. Hence Eqn. (4.22) becomes:

$$\frac{w_Q}{Q} = \left[(0.01)^2 + (0.01)^2\right]^{1/2} = 1.4142\ \% \tag{4.23}$$

4.5.3 Uncertainty in Bulk Mean Temperature

The bulk mean temperature is expressed as:

$$T_m = \frac{Q}{\dot{m}C_p} + T_{in} \tag{4.24}$$

Differentiating Eqn. (4.24), we obtain:

$$\frac{\partial T_m}{\partial \dot{m}} = \frac{-Q}{\dot{m}^2 C_p}, \tag{4.25}$$

$$\frac{\partial T_m}{\partial T_{in}} = 1 \quad \text{and} \tag{4.26}$$

$$\frac{\partial T_m}{\partial Q} = \frac{1}{\dot{m}C_p} \tag{4.27}$$

Thus, from the above equations, we get:

$$w_{Tm} = \left[\left(\frac{\partial T_m}{\partial Q} w_Q \right)^2 + \left(\frac{\partial T_m}{\partial m} w_m \right)^2 + \left(\frac{\partial T_m}{\partial T_{in}} w_{Tin} \right)^2 \right]^{1/2}$$

$$= \left[\left(\frac{w_Q}{m C_p} \right)^2 + \left(\frac{-Q}{m^2 C_p} w_m \right)^2 + \left(w_{Tin} \right)^2 \right]^{1/2} \qquad (4.28)$$

After rearranging, the uncertainty in the bulk mean temperature can be expressed as:

$$w_{Tm} = \frac{Q}{m C_p} \left[\left(\frac{w_Q}{Q} \right)^2 + \left(\frac{w_m}{m} \right)^2 + \left(\frac{m C_p}{Q} w_{Tin} \right)^2 \right]^{1/2} \qquad (4.29)$$

The relative uncertainty of the inlet temperature is taken as the accuracy of the digital thermometer which is specified as 0.25 % of reading. Again, considering the minimum flow rate, we have:

$m = 6.948546 \exp(-0.3)\ kg/s,$

$Q = 140.67 w$, and

$C_p = 1007\ J/kg^oC$

For $T_{in} = 26.5^oC$, the uncertainty becomes:

$w_{Tin} = 0.06625^oC$

Substituting the above values in Eqn. (4.26), the uncertainty in the bulk mean temperature becomes:

$$w_{Tm} = 0.9039\ ^{\circ}C \tag{4.30a}$$

Similarly, for the maximum mass flow rate with 0.9 % relative uncertainty,

$$w_{Tm} = 0.1676\ ^{\circ}C \tag{4.30b}$$

4.5.4 Uncertainties in Heat Transfer Coefficient and Nusselt Number

From Eqns. (4.8) and (4.9), the heat transfer coefficient h, is again expressed by:

$$h = \frac{\underline{Q}}{\pi DL(T_s - T_m)}$$

Differentiating the above equation, we obtain:

$$\frac{\partial h}{\partial \underline{Q}} = \frac{1}{\pi DL(T_s - T_m)} = \frac{1}{\pi DL(\Delta T)} \tag{4.31}$$

$$\frac{\partial h}{\partial T_s} = \frac{-\underline{Q}}{\pi DL(T_s - T_m)^2} = \frac{-\underline{Q}}{\pi DL(\Delta T)^2} \tag{4.32}$$

$$\frac{\partial h}{\partial T_m} = \frac{Q}{\pi DL(T_s - T_m)^2} = \frac{Q}{\pi DL(\Delta T)^2} \tag{4.33}$$

Thus, the uncertainty in the heat transfer coefficient becomes:

$$w_h = \left[\left(\frac{\partial h}{\partial Q} w_Q\right)^2 + \left(\frac{\partial h}{\partial T_s} w_{Ts}\right)^2 + \left(\frac{\partial h}{\partial T_m} w_{Tm}\right)^2\right]^{1/2} \tag{4.34}$$

Substituting the above differentials and dividing both sides by

$$h = \frac{Q}{\pi DL(T_s - T_m)},$$

The relative uncertainty in the heat transfer coefficient becomes:

$$\frac{w_h}{h} = \left[\left(\frac{w_Q}{Q}\right)^2 + \left(\frac{w_{Ts}}{\Delta T}\right)^2 + \left(\frac{w_{Tm}}{\Delta T}\right)\right]^{1/2} \tag{4.35}$$

The Nusselt number is defined by:

$$Nu = \frac{hD}{k} \tag{4.36}$$

Differentiating Eqn. (4.36), we obtain:

$$\frac{\partial Nu}{\partial h} = \frac{D}{k} \tag{4.37}$$

Therefore, the uncertainty in the Nusselt number becomes:

$$w_{Nu} = \frac{\partial Nu}{\partial h} w_h = \frac{D}{k} w_h \tag{4.38}$$

Dividing both sides of Eqn. (4.38) by Nu, we get:

$$\frac{w_{Nu}}{Nu} = \frac{w_h}{h} \tag{4.39}$$

Thus, the heat transfer coefficient and Nusselt number have equal relative uncertainties. The calibration accuracy together with maximum error in the surface temperature measuring thermometer as shown in the specification is $\pm 1.3^{o}C$. The wall-to-bulk average temperature differences encountered in the experiment centered around $\Delta T = 40^{o}C$. Hence substituting this value into Eqn. (4.35), the relative uncertainties in the heat transfer coefficient or the Nusselt number for the minimum and maximum flow rates are calculated respectively as:

$$\frac{w_h}{h} = \frac{w_{Nu}}{Nu} = \left[(0.014142)^2 + \left(\frac{1.3}{40}\right)^2 + \left(\frac{0.9039}{40}\right)^2 \right]^{1/2} = 0.04203$$

$$= 4.2\,\% \tag{4.40a}$$

and

$$\frac{w_h}{h} = \frac{w_{Nu}}{Nu} = \left[(0.014142)^2 + \left(\frac{1.3}{40}\right)^2 + \left(\frac{0.167597}{40}\right)^2 \right]^{1/2} = 0.0357$$

$$= 3.57\,\% \tag{4.40b}$$

Therefore, the average relative uncertainty in heat transfer coefficient and Nusselt number is about ± 4 %. The uncertainties in the measurements are summarized as shown in Table 4.1

Table 4.1 Uncertainties of Measurements

Parameter	**Absolute Uncertainty**	**Relative Uncertainty**
Mass flow rate		± 0.9 % to ± 4.25 %
Reynolds number		± 0.9 % to ± 4.25 %
Heat supplied		± 1.4142 %
Bulk mean temperature	$\pm 0.17\,^{\circ}C$ to $\pm$ 0.9 $^{\circ}C$	
Surface temperature	± 1.3 $^{\circ}C$	
Heat transfer coefficient		± 4.0 %
Nusselt number		± 4.0 %

CHAPTER 5

EXPERIMENTAL RESULTS AND DISCUSSION

5.1 Validation

During this study, a total of 55 tests were carried out and each pulsating test was preceded by the corresponding steady flow test at the same Reynolds number. In order to validate the experimental results, the axial variation of surface temperature and the Nusselt number for the steady flow case were compared with the data reported in the literature.

The measured surface temperature distribution corresponding to a wide range of Reynolds number is shown in Fig. 5.1. As can be seen, the pattern of the surface temperature distribution agrees very well with the published patterns [8] for thermal entrance forced convection heat transfer in pipes heated with uniform heat flux .

Also the values of Nusselt number in the thermally fully developed region were compared with those reported in the literature [8]. As shown in Fig. 5.2, these values were found to be in very good agreement with Dittus-Boelter correlation presented in [8] and given as:

$$Nu = 0.023\, Re^{0.8}\, Pr^{0.4} \qquad (5.1)$$

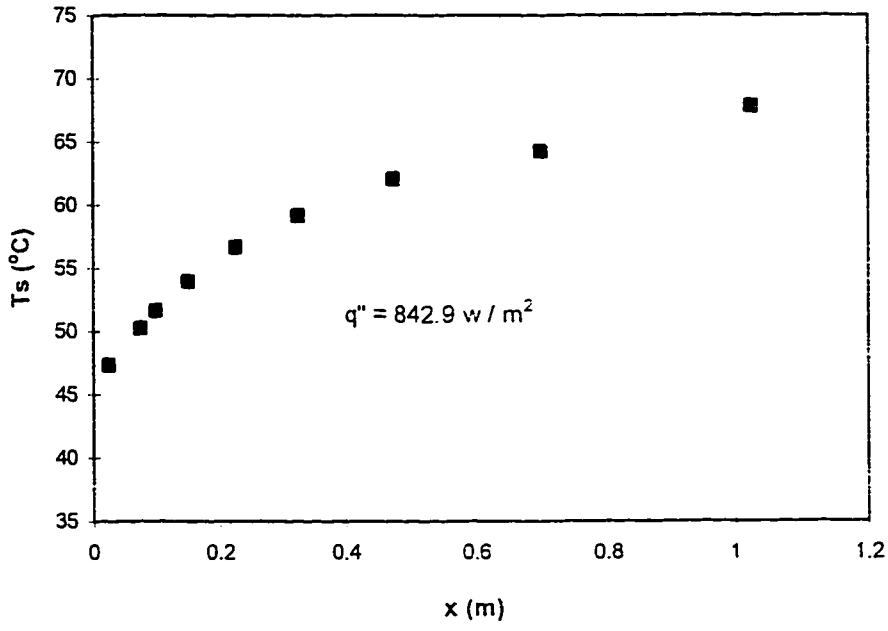

Fig. 5.1a Steady flow surface temperature distribution
(Re = 19950)

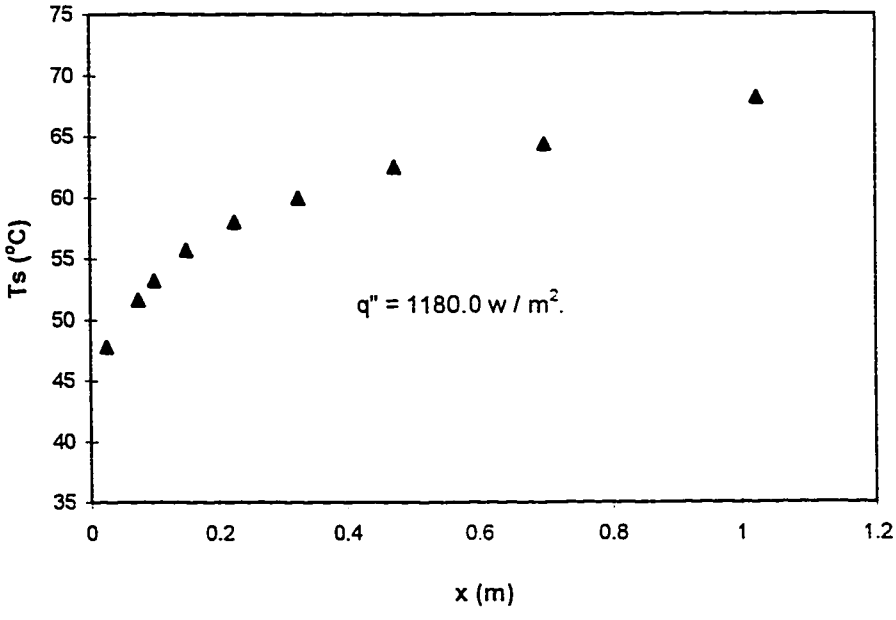

Fig .5.1b Steady flow surface temperature distribution
(Re = 33663)

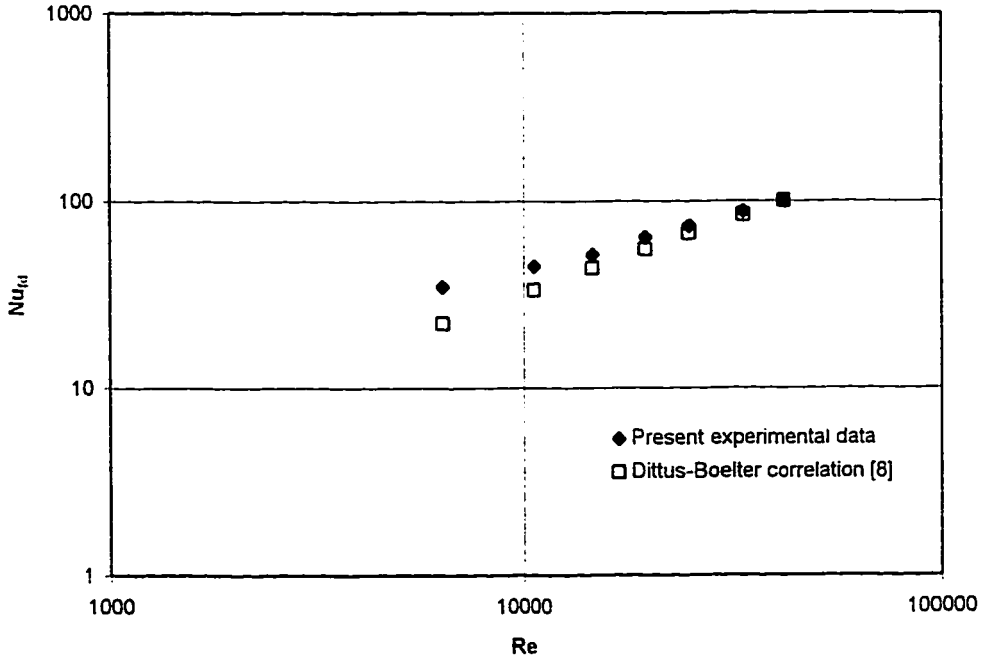

Fig. 5.2 Comparison of experimental fully developed Nusselt numbers with Dittus-Boelter correlation [8]

The comparison shows a difference of about 5 % and 1 % for Reynolds number of 33663 and 41947 respectively. The considerable difference between the two Nusselt numbers at Re = 6387 may be due to the fact that the correlation is valid for Reynolds number in the range between 10^4 and 10^5.

5.2 Discussion of Results

The effect of pulsation on heat transfer will be assessed by obtaining the ratio of the heat transfer coefficient or Nusselt number under the influence of pulsation to the corresponding steady values for flow without pulsation. This ratio is referred to as relative Nusselt number.

5.2.1 Relative Local Nusselt Numbers

Since the present work is devoted to study the effect of pulsation in the thermal entrance region of a hydrodynamically fully developed turbulent air flow in a pipe, it becomes pertinent to examine the behavior of the local Nusselt number along the test section, under the influence of pulsation. The relative local Nusselt number is defined as the ratio of the value of local Nusselt number for pulsed flow to the corresponding one for steady flow (without pulsation) at the same Reynolds number. The relative local Nusselt number variation along the pipe for different flow Reynolds numbers at different pulsation frequencies are shown in Figs. 5.3(a to h). It is observed to some extent,

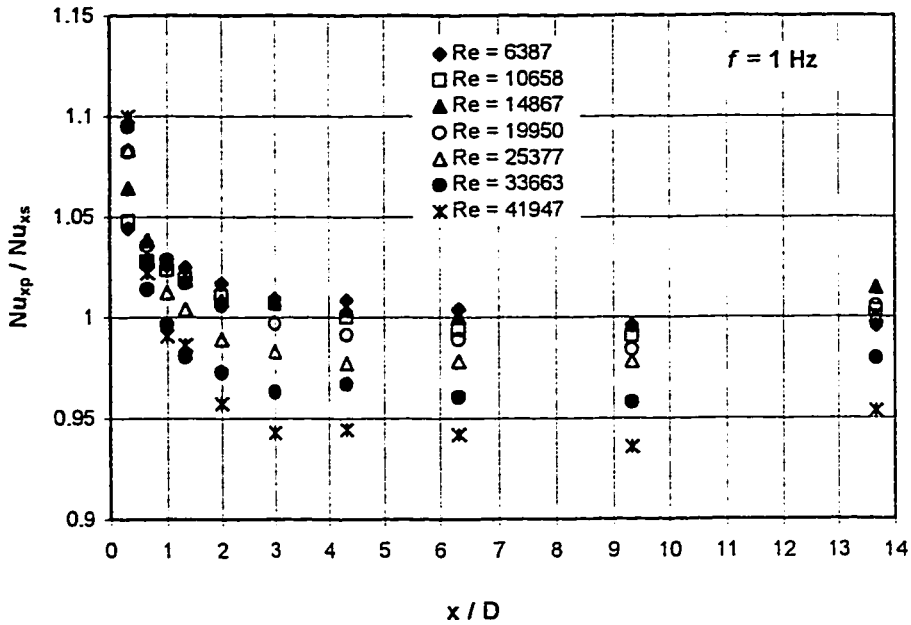

Fig. 5.3a Effect of pulsation on local Nusselt numbers at different flow Reynolds numbers

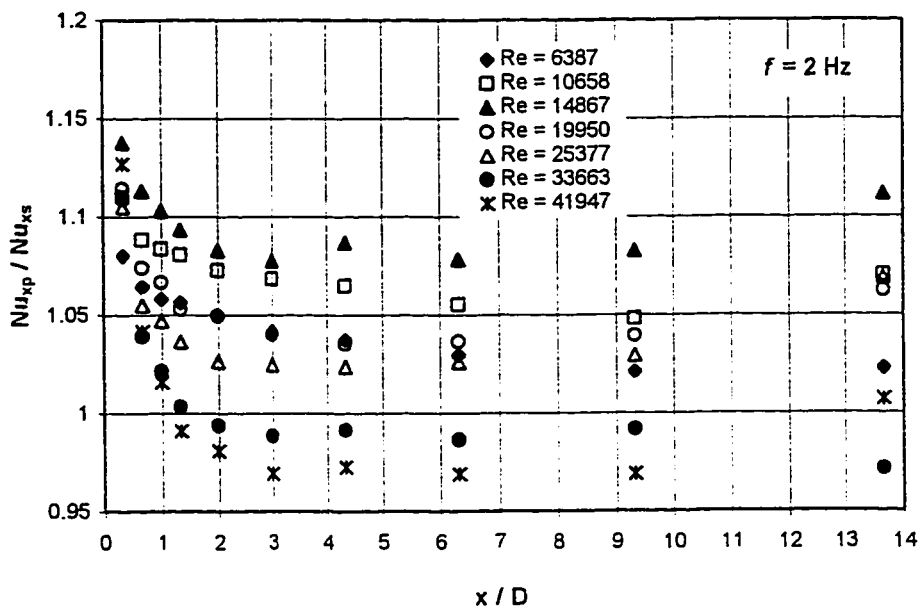

Fig. 5.3b Effect of pulsation on local Nusselt numbers at different flow Reynolds numbers

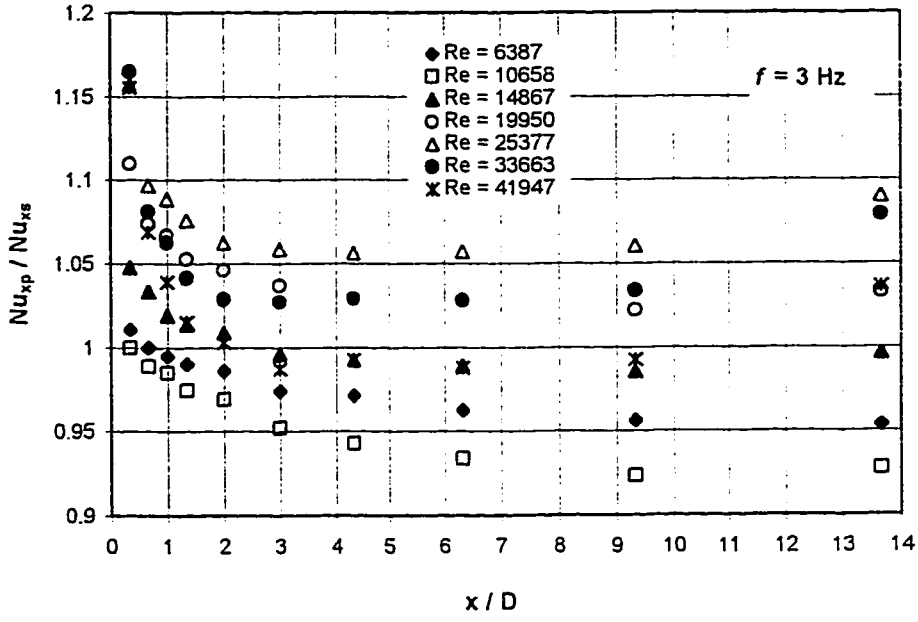

Fig. 5.3c Effect of pulsation on local Nusselt numbers at different flow Reynolds numbers

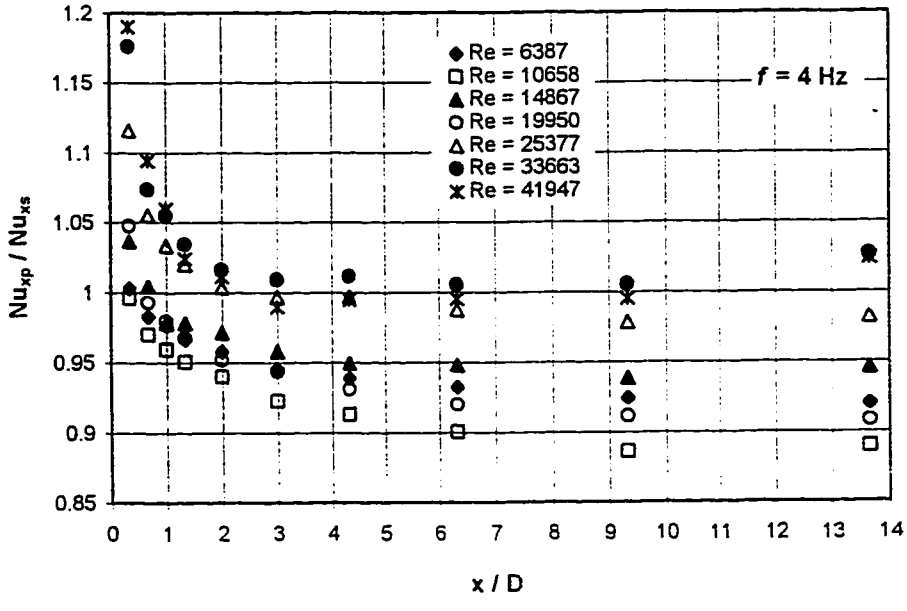

Fig. 5.3d Effect of pulsation on local Nusselt numbers at different flow Reynolds number

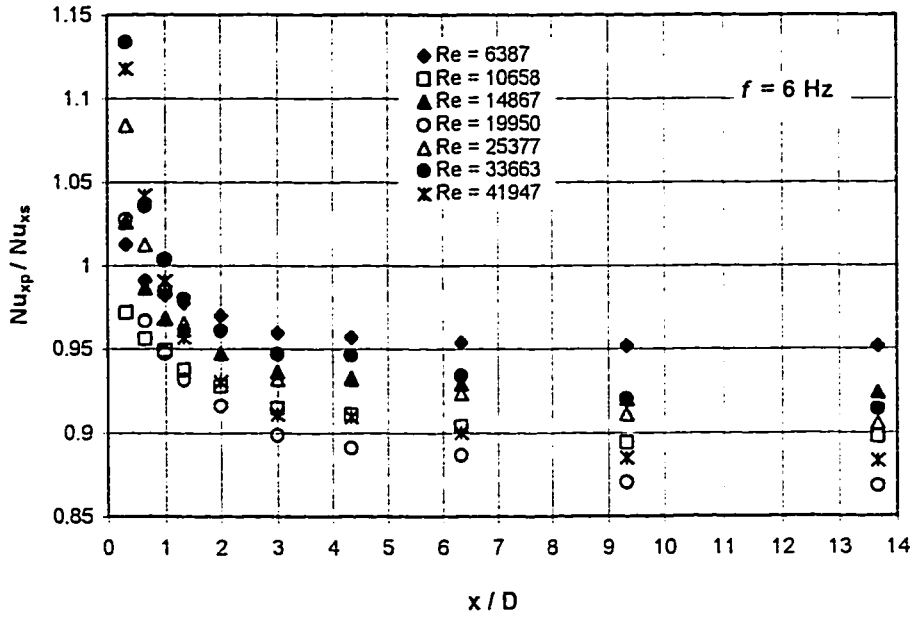

Fig. 5.3e Effect of pulsation on local Nusselt numbers at different flow Reynolds numbers

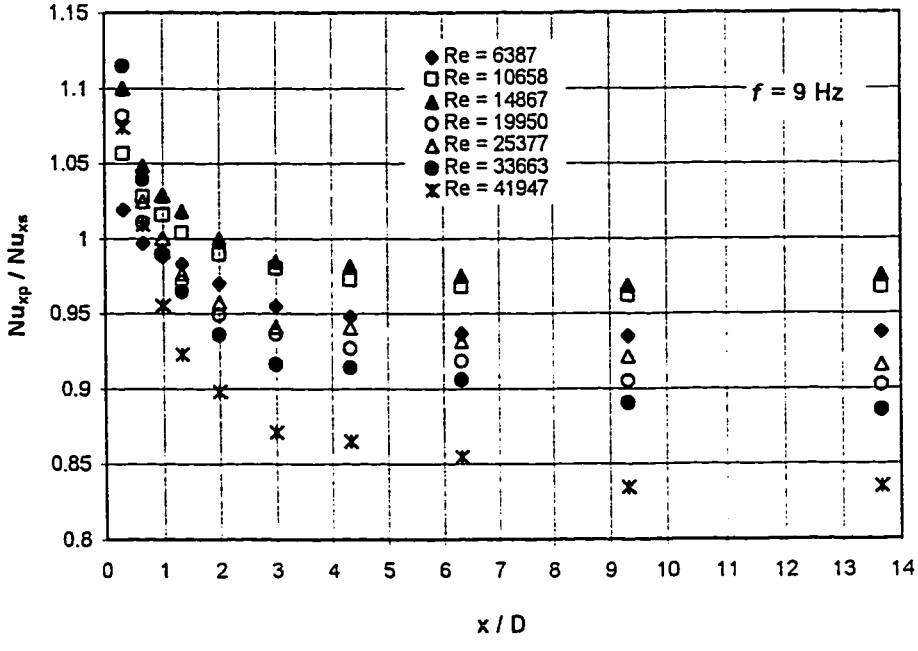

Fig. 5.3f Effect of pulsation on local Nusselt numbers at different flow Reynolds numbers

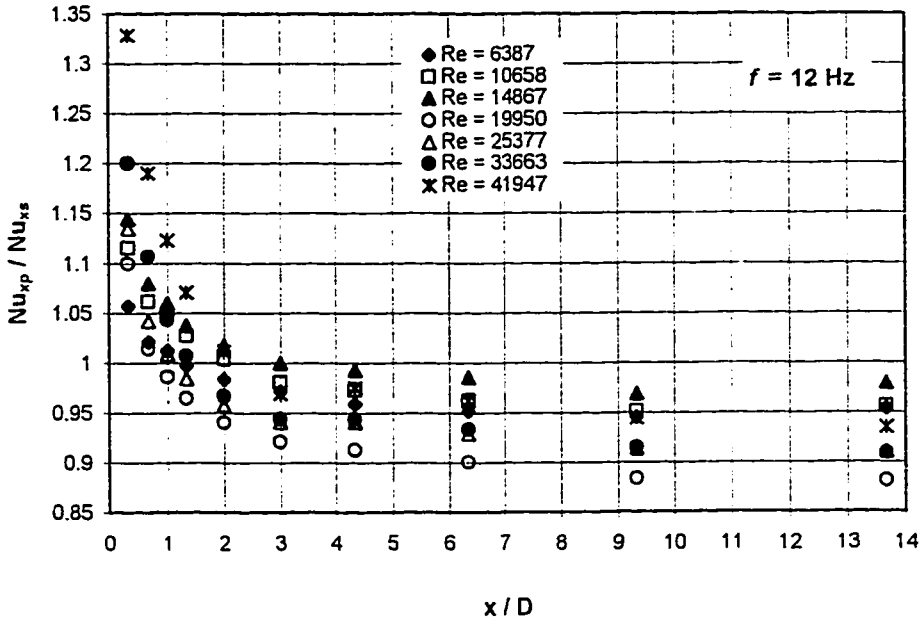

Fig.5.3g Effect of pulsation on local Nusselt numbers at different flow Reynolds numbers

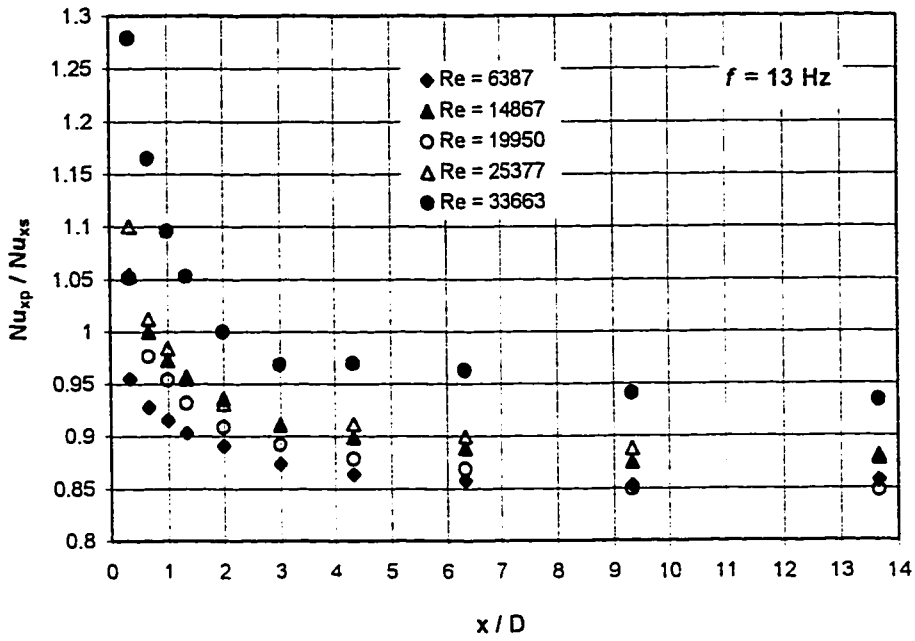

Fig. 5.3h Effect of pulsation on local Nusselt numbers at different flow Reynolds numbers

that the relative local Nusselt numbers exhibit pattern similar to that of steady flow. This may be due to the observed similar pattern of surface temperature distribution for the two cases. As can be seen from the figures, local heat transfer enhancement is observed close to the inlet. Pulsation frequency of 1 Hz (Fig. 5.3a) produces enhancement at Reynolds number less than or equal to 14867 and extends down to a length of about 4 pipe diameters. However, reduction in heat transfer coefficient is observed along the test section for Re greater than 14876. Enhancement was observed along the entire test section for Re up to 25377 at a pulsation frequency of 2 Hz as shown in Fig. 5.3b. Enhancement is high both at the inlet and downstream the test section with maximum increase of about 14 %, close to the inlet and 11 % at the exit for Reynolds number of 14867. Similar pattern was exhibited at a pulsation frequency of 3 Hz and a range of Reynolds number from 14867 to 33663, as shown in Fig. 5.3c. In this case, heat transfer enhancement is observed along the entire test section, increasing up to 16 % near the inlet and 9 % at the exit of the test section for Reynolds number of 25377. However, as can be observed from Figures 5.3d to 5.3h, pulsation at frequencies equal to or higher than 4 Hz results in reduction in the local Nusselt numbers along the test section for all the Reynolds numbers. Here, relative enhancement is confined only very close to the inlet between 1 and 2 pipe diameters length with maximum value of about 34 % near the inlet at Reynolds number of 41947. The reason for the considerable local enhancement close to the inlet may be

due to strong agitation of the thermal boundary layer (whose growth has just begun) by the imposed pulsation.

5.2.2 Relative Mean Nusselt Numbers

The mean Nusselt numbers for steady and corresponding pulsating flows at different frequencies considered in the experiment are summarized in Table 5.1. The steady flow values shown for the mean Nusselt number are the arithmetic average of the readings (that preceded flow pulsation) at the same Reynolds number. The values are within a difference of 1 %.

Figures (5.4a, b, and c) show the overall relative mean Nusselt number as a function of the pulsation frequency for Reynolds numbers ranging from 6387 to 41947. One can observe that all the curves show almost similar trend. As can be seen, maximum heat transfer enhancement of about 9 % is obtained at a frequency of 2 Hz and Re = 14867. Enhancement frequency range is between 1.5 Hz and 2.5 Hz for curves corresponding to Reynolds number from 6387 to 14867 with maximum enhancement occurring at 2 Hz as shown in Fig. 5.4a. For Reynolds number 19950 and 25377 (Fig 5.4b), the enhancement frequency band increases slightly and lies between 1.5 Hz and 3.5 Hz. In this case, maximum enhancement of about 7 % occurs at a pulsation frequency of 3 Hz, for Reynolds number of 25377. Also, there is little enhancement of about 4 % occurring at the same pulsation frequency of 3 Hz for Reynolds

Table 5.1 Summary of Experimental Results

Re	Mean Nusselt Number								
	Steady Flow	Pulsating Flow Frequency *f* (Hz)							
		1	2	3	4	6	9	12	13
6387	35.675	35.827	36.83	34.467	33.469	34.427	33.879	34.396	31.014
10658	45.222	45.113	48.263	42.741	41.254	40.955	43.944	43.909	39.685
14867	54.075	54.092	58.51	53.505	51.227	50.184	52.889	53.421	49.087
19950	66.48	66.608	69.843	69.05	62.073	59.533	61.405	60.363	58.163
25377	77.836	76.774	80.511	82.976	77.266	72.541	73.316	73.188	70.998
33663	92.5	90.455	93.306	97.195	94.893	87.836	84.44	89.268	91.759
41947	107.557	102.332	105.771	108.2	108.597	98.024	93.248	105.64	-

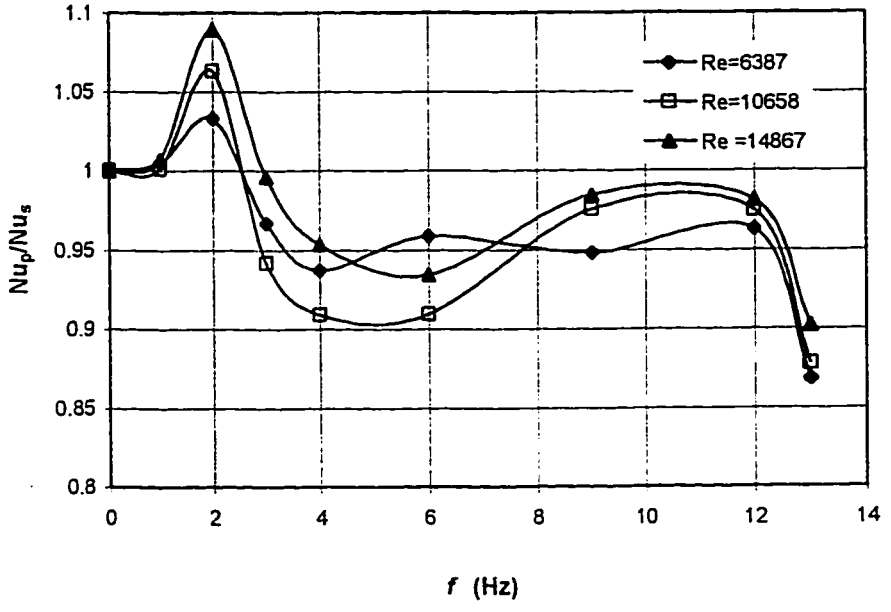

Fig. 5.4a Relative mean Nusselt number as a function of pulsation frequency

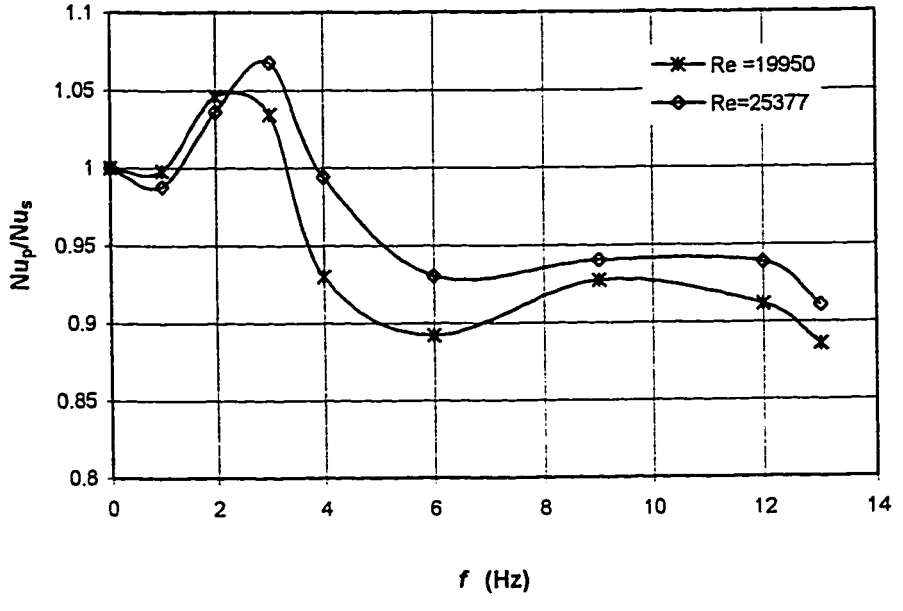

Fig. 5.4b Relative mean Nusselt number as a function of pulsation frequency

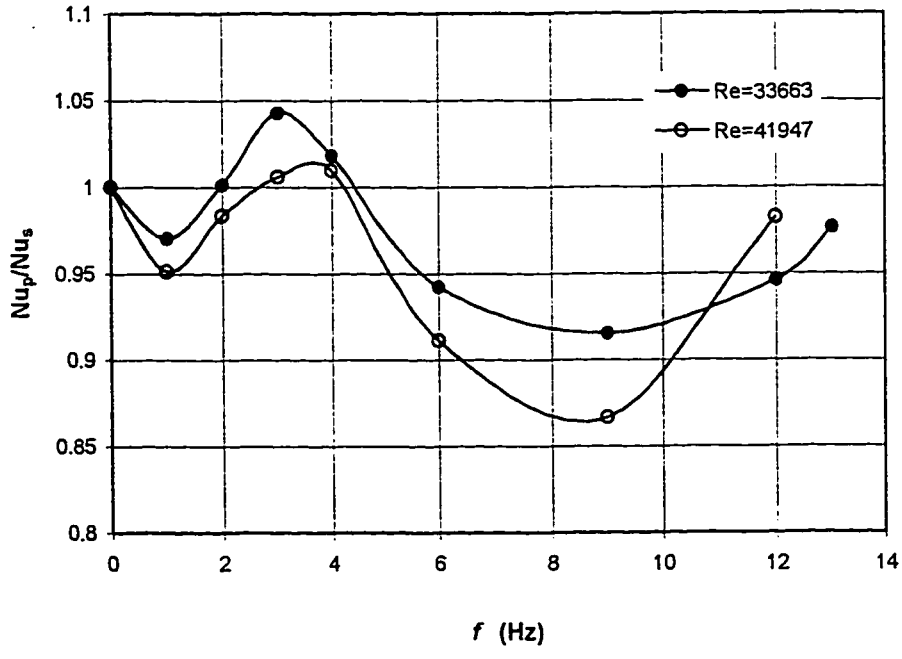

Fig. 5.4c Relative mean Nusselt number as a function of pulsation frequency

number of 33663 while little or negligible enhancement was observed at frequency of 4 Hz for Reynolds number of 41947 as shown in Fig. 5.4c.

It is interesting to note that when frequency of pulsation increases, ($f > 4$ Hz), reduction in the overall heat transfer coefficient is observed for the whole range of Reynolds numbers considered in this study. For example, a maximum reduction of about 13 % did occur at 9 Hz for Re = 41947. On the other hand, it can also be observed that, for Reynolds numbers in the range of 10000 to 20000, there is an increase in the relative mean Nusselt number for the pulsation frequency range of 6 Hz to 9 Hz. Within this frequency range, maximum increase of 7.3 % is recorded at Reynolds number of 10658. Also, the relative mean Nusselt number remains nearly constant in the same pulsation frequency range of 6 Hz to 9 Hz for Re = 25377 (see Fig. 5.4b). For high Reynolds numbers, the relative mean Nusselt number decreases (in the frequency range of 4 Hz to 9 Hz) and it starts to increase again beyond this frequency range as seen in Fig. 5.4c.

Figures (5.5a, b, c and d) show the plots of relative mean Nusselt number versus the flow Reynolds numbers for different values of pulsation frequencies. Also shown in Fig. 5.6 is the plot of maximum enhancement values obtained in this study at different Reynolds numbers. These graphs act as prediction charts whereby for a given flow, one can predict the pulsation frequencies at which enhancement or reduction in the heat transfer coefficient (relative to the steady flow value) can be obtained. For example, maximum enhancement is achieved

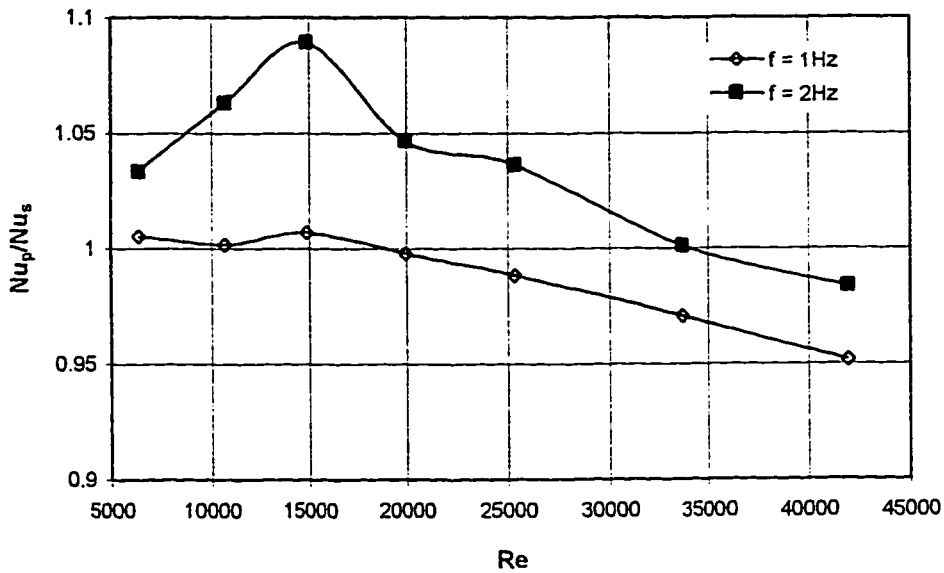

Fig. 5.5a Relative mean Nusselt number as a function of flow Reynolds number

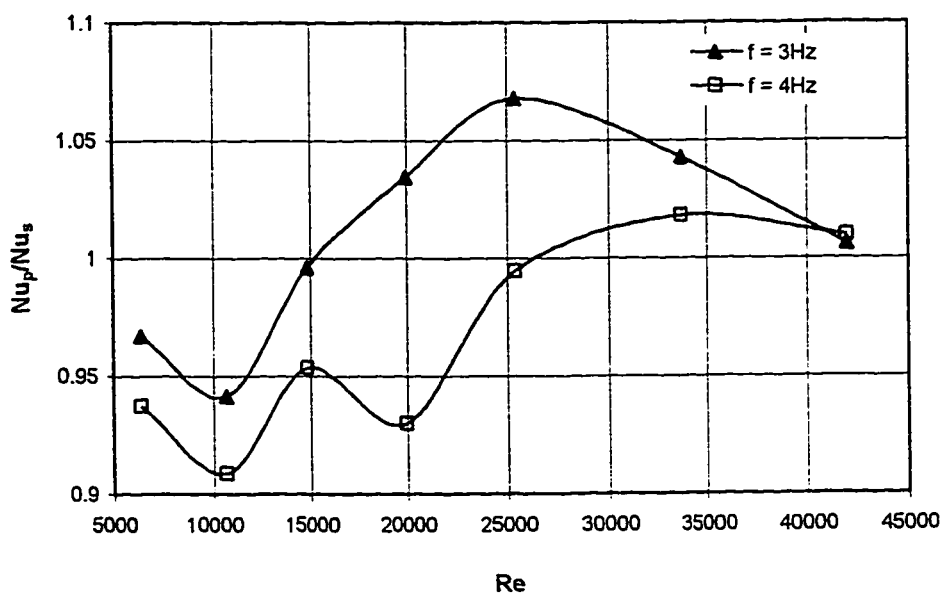

Fig. 5.5b Relative mean Nusselt number as a function of flow Reynolds number

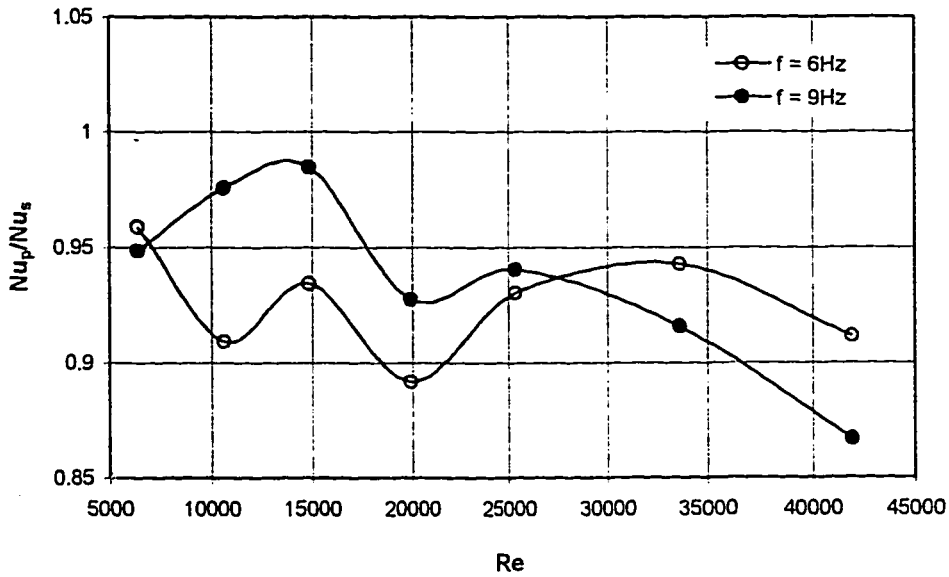

Fig. 5.5c Relative mean Nusselt number as a function of flow Reynolds number

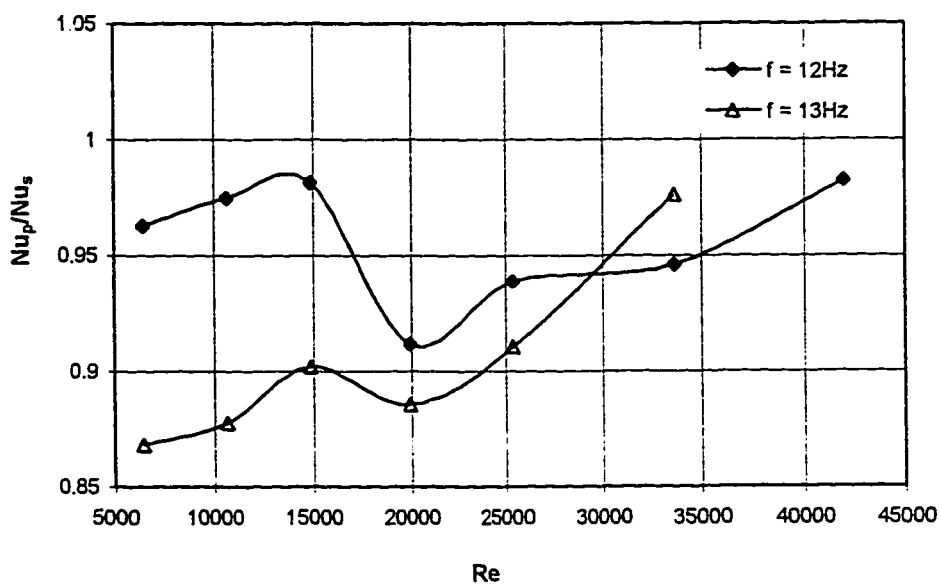

Fig. 5.5d Relative mean Nusselt number as a function of flow Reynolds number

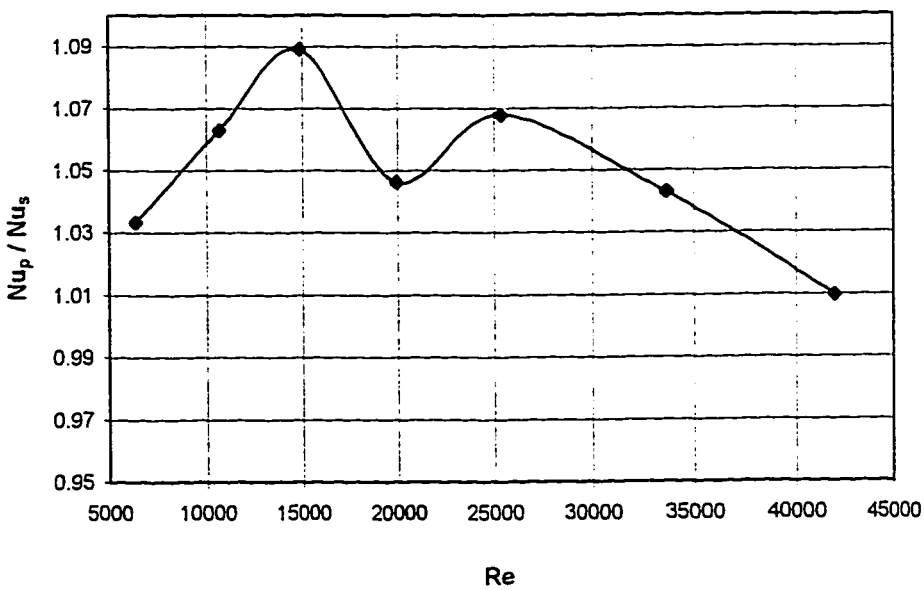

Fig.5.6 Maximum enhancement values of the relative mean Nusselt number

at a pulsation frequency of 2 Hz for Reynolds number in the range 6000 to 20000. However, maximum enhancement is achieved at a pulsation frequency of 3 Hz for the Reynolds number in the range of 19000 to 35000 as shown in Fig. 5.6. Another striking feature of these figures is that at high Reynolds number, the effect of pulsation on heat transfer becomes negligible. This can be attributed to the fact that at these Reynolds numbers, the flow is highly turbulent and the turbulent intensity is probably having a more dominant effect on the flow compared to the imposed pulsation. The observed reduction in the average heat transfer coefficient as frequency of pulsation increases may be as a result of enhancement of turbulence due to the high frequency. The velocity amplitude of the oscillating piston of the pulsating mechanism has been found to increase with the frequency as shown in Fig. 3.4. This therefore leads to further enhancement of turbulence which might lead to a more dominant role compared to pulsation.

5.2.3 Analysis of Data on Heat Transfer with Pulsating Flow in Relation to Bursting Phenomenon

The effect of pulsation on the mass flow rate has been found to be related to the bursting process of the turbulent boundary layer [35, 36]. As discussed in Chapter 2 the importance of bursting process in turbulent energy production makes it also essential to turbulent heat transfer. With such analogy, data on

heat transfer with pulsating flow have been discussed using the turbulent bursting model [4,15]. Hence, the present experimental results will be discussed in relation to turbulent bursting process. To carry out such a discussion, Fig. 2.1 is replotted as shown in Fig. 5.7 but now with classification of the present data (represented by boundaries of the data) as well as data of other investigators. As can be seen, the bulk of the present data fall into the preferred range of the bursting frequencies (regimes B and C). It is also observed that pulsation frequencies at which overall heat transfer enhancement occurs are very close to the mean bursting frequency line. It is apparent that increase in heat transfer coefficient is presumably the result of changes in the mean bursting frequencies which are now controlled by the imposed pulsation frequencies. Therefore based on this model, critical frequencies at which resonance interaction between the bursting frequencies and those of imposed pulsation are likely to have occurred are in the neighborhood of 2 Hz and 3 Hz respectively.

This model has been able to predict the results of other investigators such as **Haveman and Rao** [11] and **Liao et al.**[4]. The data reported in [11] lies in the preferred range which agrees with their findings that the Nusselt number is increased for pulsation frequency above a certain value and is decreased below it. Also, the data reported by [4] fall on the 'low-frequency regime' (regime A) outside the preferred range where the mean bursting frequency is independent of pulsation frequency and as reported, their result showed no dependence of frequency as well as reduction in heat transfer coefficient.

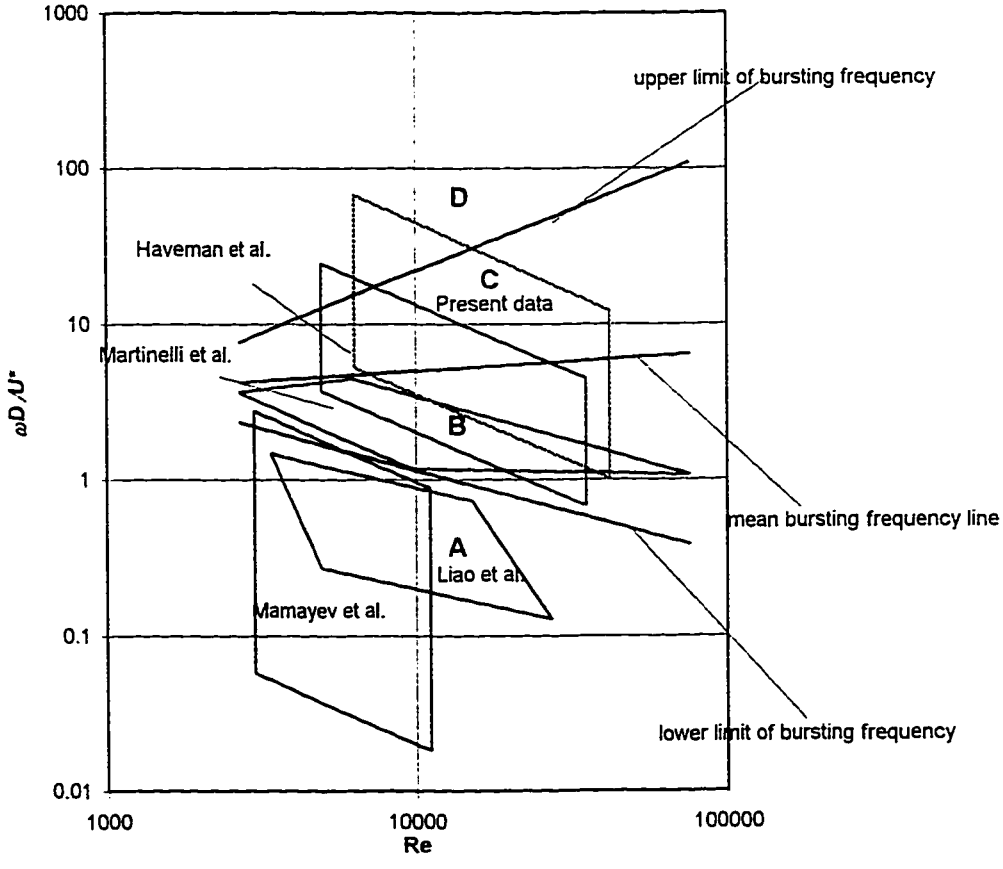

Fig.5.7 Classification of data on heat transfer with pulsating turbulent pipe flow.

It is worth pointing out that the findings of some investigators such as **Martinelli et al** [10] and **Mamayev et al** [5] did not match this concept. The data of **Martinelli et al.** [10] fall in the 'intermediate frequency regime' (regime B) of the range of bursting frequencies where heat transfer is expected to be affected by the imposed pulsation frequencies. However as their result showed, overall heat transfer coefficient was not affected by the pulsation. This is probably due to the fact a semi-sinusoidal pulsation was imposed on the flow [4]. In the case of **Mamayev et al** [5], their frequency range lies outside the preferred range in regime A, below the lower limit of turbulent bursting frequency where $\omega D / U^* << 1$ and as a result, the flow is expected to exhibit quasi-steady behavior [36]. Here the process of heat transfer like that of turbulent bursting frequency should be independent of pulsation frequency but depend on the amplitude [4]. However their results, as reviewed in chapter 2 showed a considerable dependence on frequency as well as increase in the heat transfer coefficients.

In summary, the model of turbulent bursting has been able to provide fairly logical explanation regarding the results of the present study as well as other studies of heat transfer in pulsating flows. However, it is also noted that some experimental results contradict the classification as discussed above. The studies of **Ramaprian and Tu** [36] and those of other investigators on which the classification is based, were carried out with pulsating flows of certain wave

forms, hence, the effect of wave form on pulsating flows may play a key role in providing the reason why some results do or do not conform with the model predictions.

CHAPTER 6

CONCLUSIONS AND RECOMMENDATIONS

6.1 SUMMARY AND CONCLUSIONS

The effect of pulsation frequency on heat transfer coefficient in the thermal entrance region of a hydrodynamically fully developed turbulent air flow in a pipe heated with a uniform heat flux has been experimentally studied. The flow Reynolds number was varied from 6387 to 41947. A near sinusoidal pulsation (originating downstream from the pipe exit) with frequency ranging from 1 Hz to 13 Hz was imposed on the flow. Although, the mean Nusselt number has been found to depend on the imposed frequency, the results showed (to some extent) pattern similar to steady flow, of variation of the local Nusselt number along the pipe.

Enhancement of the overall heat transfer coefficient was observed only at pulsation frequencies of 2 Hz and 3 Hz. From the range of Reynolds number covered, enhancement at 2 Hz were observed from low to medium Reynolds number with a maximum of 9 % recorded at Re near 15000. For medium to higher Reynolds number, increase in the Nusselt number was observed at a pulsation frequency of 3 Hz but this time with a maximum of 7 % at Reynolds number slightly above 25000. On the other hand, at frequencies of pulsation greater

than 4 Hz, a reduction in the average heat transfer coefficient was observed for all the range of Reynolds number considered in the experiment. This reduction is not directly proportional to the frequency as there was a relative increase in the mean Nusselt number as frequency increased from 6 Hz to 9 Hz for Reynolds numbers less than or equal to 25000 and as it increased from 9 Hz to 12 Hz for higher Reynolds numbers.

Observation of the local Nusselt number behavior under the influence of pulsation revealed that improvement is more pronounced close to the inlet as well as towards the exit of the test section at those frequencies that yielded overall enhancement. However at other frequencies, enhancement still exists near the inlet while reduction dominates downstream.

Also, based on the bursting bursting process, it can be concluded that critical frequencies where resonance interaction between the bursting and pulsating frequencies occur are in the neighborhood of 2 Hz and 3 Hz.

It is interesting to note that despite the enhancement or reduction recorded, the uncertainty in the mean Nusselt number was about 4 % (see section 4.5). Therefore, by comparing the maximum enhancement of 9 % to this level of uncertainty, one can reasonably speculate that flow pulsation contributes less significantly to the already high heat transfer coefficient in the thermally developing region of pipe flows. In general, one also should note that the

maximum possible heat transfer in steady internal flows takes place in this region of thermal boundary layer development.

6.2 RECOMMENDATIONS FOR FUTURE WORK

As an extension to the present work, it is recommended to account for the following flow pulsation parameters:

1. Variation in the displacement amplitude of pulsation inducing mechanism especially at very low frequencies of the order $f < 0.5$ Hz. This may have an effect on the heat transfer coefficient observed at such frequency. [4].
2. Location of the pulsator such as upstream the test section. This has also been found to have effect on the heat transfer coefficient [13,18].
3. Mode and pulsation wave form: a tangential rather than axial pulsation may exhibit certain influence on the heat transfer behavior in the test section. Also pulsation of different wave-forms can be devised.

As far as the flow and fluid parameters are concerned the following recommendations are also essential as an extension to the present work:

1. Investigation of laminar thermal entrance flow under the influence of pulsation as well as transition and turbulent flows at Reynolds numbers outside the present range.
2. Extension of the work to cover the effect of Prandtl number by testing different fluids

APPENDIX

DATA REDUCTION SAMPLE PROGRAM AND OUTPUT

```
      Dimension x(12),ts(12),tm(12),h(12),rnu(12)
      Open(unit= 5,file='NusseltG.dat')
      Open(unit= 6,file='NusseltG.out')
      pi = 3.1415927
      cp = 1007.0
      rmair = 0.00001846
      rholiq = 827.0
      rhowat = 1000.0
      rhoair = 1.1614
      conduc = 0.0263
      condis = 0.035
      dtests = 0.0750316
      dorfce = 0.0780161
      dorfc2 = 0.0613918
      gravty = 9.81
      tstlgt = 1.025
      coeffd = 0.6251095
      Aorfce = (pi*dorfc2 **2.0)/ 4.0
      Atests = (pi*dtests **2.0)/4.0
c     ******Enter the manometer reading***********
      Read(5,*) deltah
      Deltq = (rhowat/rhoair - 1.0)*deltah
      vpipe = sqrt(2*gravty*Deltq)
c     *Calculate mass flow rate and Reynolds number at test section*
      rmdot = coeffd*rhoair*Aorfce*vpipe
      reyno = 4*rmdot/(pi*dtests*rmair)
      vavrg = rmdot/(rhoair*Atests)
c     ****Enter the heat input and calculate the total heat flux****
      Read(5,*) power
      qtotal = 5.0*power
      qdotot = qtotal/(pi*din*1.18)
      qtranst = 0.9378*qtotal
c     ****************Enter the surface temperatures***************
      Do 9 i = 1,11
      Read(5,*) x(i),ts(i)
    9 continue
c     **************Calculate the bulk mean temperatures************
```

```
      tbin = ts(1)
      Tbulk = qtranst/(rmdot*cp) + tbin
      Do 15 i = 2,11
      tm(i) = (Tbulk - tbin)*(x(i) - x(1))/1.18 +tbin
   15 Continue
      qdot = qtranst/(pi*dtests*1.18)
      tqlost = qtotal - qtranst
c     ***Calculate the local and average heat transfer coefficients**
      Do 20 i = 2, 11
      h(i) = qdot/(ts(i) - tm(i))
      rnu(i) = h(i) * dtests/conduc
   20 Continue
      hm1=(x(2)/2.)*(h(2)+h(5)) + x(2)*(h(3)+h(4))
      hm2=(x(3)/2.)*(h(5)+h(6)) + (x(4)/2.)*(h(6)+h(7))
      hm3=(x(5)/2.)*(h(7)+h(8)) + (x(6)/2.)*(h(8)+h(9))
      hm4=(x(7)/2.)*(h(9)+h(10)) + (x(8)/2.)*(h(10)+h(11))
      hmean = (hm1 + hm2 + hm3 + hm4)/1.025
      rnum = hmean * dtests/conduc
      write(6,*)
      Read(5,*) freq
      if(freq.eq.0.0)go to 29
      Write(6,*)'Heat Transfer to Pulsed Flow,Freq. equal to',freq,' Hz'
      Go to 31
   29 Write(6,*)'Steady State Solution of Flow without Pulsation'
   31 Write(6,*)
      Write(6,*)'Re =',reyno,'  Mean Nusselt No.=',rnum
      Write(6,*)
      Write(6,*)'Inlet Temp.=',tbin,' deg.C'
      Write(6,*)
      write(6,*)'  x(m) ','   Tmean(x)','   Tsurf(x)','    h(x)'
     &,'   Nu(x) '
      Write(6,*)
      Do 25 i = 2, 11
      write(6,30) x(i),tm(i),ts(i),h(i),rnu(i)
   30 format (f6.3,3x,4f11.5)
   25 continue
      Write(6,*)
      write(6,*)'Flowrate=',rmdot,' kg/s',' Average veloc=',vavrg,' m/s'
      Write(6,*)
      write(6,*)'Heat Input=',qtotal,'w',' Heat transfered=',qtranst,'w'
      write(6,*)
      write(6,*)'Average temp. downstream is',Tbulk,' deg.C'
      write(6,*)
      end
```

Steady State Solution of Flow without Pulsation

Re = 14867.37 Mean Nusselt No.= 53.716070
Inlet Temp.= 21.60 deg.C

x(m)	Tmean(x)	Tsurf(x)	h(x)	Nu(x)
0.025	21.78299	41.60000	25.52039	72.80745
0.050	21.96598	43.60000	23.37697	66.69246
0.075	22.14897	43.60000	23.57639	67.26139
0.100	22.33196	44.60000	22.71138	64.79358
0.150	22.69795	46.20000	21.51888	61.39148
0.225	23.24692	48.20000	20.26755	57.82155
0.325	23.97889	50.30000	19.21415	54.81629
0.475	25.07683	52.60000	18.37499	52.42223
0.700	26.72375	54.30000	18.33962	52.32132
1.025	29.10264	57.00000	18.12852	51.71907

Flowrate= 1.617335E-02 kg/s Average veloc= 3.149487 m/s
Heat Input= 150.00 w Heat transfered= 140.67 w
Average temp. downstream is 30.237180 deg.C

Heat Transfer to Pulsed Flow,Freq. equal to 1.00 Hz

Re = 14867.37 Mean Nusselt No.= 54.092390
Inlet Temp.= 21.20 deg.C

x(m)	Tmean(x)	Tsurf(x)	h(x)	Nu(x)
0.025	21.38299	40.00000	27.16536	77.50040
0.050	21.56598	42.40000	24.27462	69.25336
0.075	21.74897	42.60000	24.25482	69.19688
0.100	21.93196	43.80000	23.12681	65.97876
0.150	22.29795	45.60000	21.70358	61.91840
0.225	22.84692	47.60000	20.43131	58.28874
0.325	23.57889	49.80000	19.28743	55.02534
0.475	24.67683	52.20000	18.37498	52.42223
0.700	26.32375	54.00000	18.27335	52.13227
1.025	28.70264	56.20000	18.39223	52.47143

Flowrate= 1.617335E-02 kg/s Average veloc= 3.149487 m/s
Heat Input= 150.00 w Heat transfered= 140.67 w
Average temp. downstream is 29.837180 deg.C

Heat Transfer to Pulsed Flow, Freq. equal to 2.00 Hz

Re = 14867.37 Mean Nusselt No.= 58.509480
Inlet Temp.= 21.20 deg.C

x(m)	Tmean(x)	Tsurf(x)	h(x)	Nu(x)
0.025	21.38299	38.80000	29.03701	82.84005
0.050	21.56598	41.00000	26.02333	74.24228
0.075	21.74897	41.20000	26.00057	74.17735
0.100	21.93196	42.30000	24.82998	70.83775
0.150	22.29795	44.00000	23.30369	66.48338
0.225	22.84692	46.00000	21.84322	62.31680
0.325	23.57889	47.80000	20.88004	59.56893
0.475	24.67683	50.20000	19.81485	56.53004
0.700	26.32375	51.80000	19.85135	56.63416
1.025	28.70264	53.80000	20.15104	57.48915

Flowrate= 1.617335E-02 kg/s Average veloc= 3.149487 m/s
Heat Input= 150.00 w Heat transfered= 140.67 w
Average temp. downstream is 29.84 deg.C

Heat Transfer to Pulsed Flow,Freq. equal to 3.00 Hz

Re = 14867.37 Mean Nusselt No.= 53.504880
Inlet Temp.= 21.50 deg.C

x(m)	Tmean(x)	Tsurf(x)	h(x)	Nu(x)
0.025	21.68299	40.60000	26.73456	76.27135
0.050	21.86598	42.80000	24.15866	68.92254
0.075	22.04897	43.10000	24.02438	68.53945
0.100	22.23196	44.20000	23.02153	65.67841
0.150	22.59795	45.90000	21.70357	61.91839
0.225	23.14692	48.20000	20.18665	57.59075
0.325	23.87889	50.40000	19.06925	54.40290
0.475	24.97683	52.80000	18.17686	51.85699
0.700	26.62375	54.60000	18.07740	51.57324
1.025	29.00264	57.00000	18.06377	51.53435

Flowrate= 1.617335E-02 kg/s Average veloc= 3.149487 m/s
Heat Input= 150.00 w Heat transfered= 140.67 w
Average temp. downstream is 30.137180 deg.C

NOMENCLATURE

a	: Lower part of link 2 of pulsating mechanism (m)
A	: Pulsation amplitude
A_o	: Area of orifice (m^2)
A_r	: Heat transfer area (m^2)
b	: Upper part of link 2 of pulsating mechanism (m)
B	: Relative velocity oscillation amplitude
c	: Crank length of pulsating mechanism (m)
C_d	: Orifice discharge coefficient
C_p	: Specific heat capacity of fluid (J/Kg.^oC)
D	: Pipe diameter (m)
f	: Frequency of pulsation (Hz)
f_b	: Turbulent bursting frequency (Hz)
g	: Acceleration due to gravity (m/s^2)
Δh	: Height of manometer liquid (m)
h_{mean}	: Mean heat transfer coefficient (w/m^2K)
$h(x)$	: Local heat transfer coefficient (w/m^2K)
H	: Half channel width (m)
I	: Electric current supplied (Amps)
k	: Thermal conductivity of fluid (w/mK)

l	: Length of link 2 of pulsating mechanism (m)
L	: Length of test section (m)
L_e	: Effective length of test section (m)
L_s	: Length of slider of pulsating mechanism (m)
m	: Mass flow rate (kg/s)
M	: Frequency parameter, $\left(\omega H^2/2\upsilon\right)^{\frac{1}{2}}$
n	: Characteristic constant for quasi-steady model
Nu_m	: Mean Nusselt number (time average)
Nu_x	: Local Nusselt number (time average)
$\frac{Nu_p}{Nu_s}$	: Relative mean Nusselt number (time average)
$\frac{Nu_{xp}}{Nu_{xs}}$	: Relative local Nusselt number (time average)
Pr	: Prandtl number
$\dot{q}_{loss}$	: Heat flux loss in heater segment (w/m^2)
$\dot{q}_o$	: Total heat flux (w/m^2)
q_{trans}	: Heat transferred from heater segment (w)
Q_{loss}	: Total heat loss (w)
Q	: Heat input (w)
Q_{trans}	: Total heat transferred (w)
r	: Local pipe radius (m)

R_{cs}	: Radius of inner surface of insulation (m)
R_{cso}	: Radius of outer surface of insulation (m)
Re	: Reynolds number
t	: Pipe thickness (m)
T_{cso}	: Local outer surface temperature of insulation (°C)
T_{cs}	: Local inner surface temperature of insulation (°C)
T_s	: Pipe surface temperature (°C)
$T_s(x)$	: Local pipe surface temperature (°C)
T_{bulk}	: Bulk fluid temperature (°C)
T_{in}	: Fluid inlet temperature (°C)
$T_b(x)$	: Local bulk mean temperature (°C)
U^*	: Friction velocity (m/s)
V	: Voltage supplied (V)
V_m	: Time averaged velocity (m/s)
V_p	: Sinusoidal velocity of pulsation inducing piston (m/s)
V_s	: Steady velocity component (m/s)
x	: Local distance along the test section (m)
x	: Displacement of link 2 of pulsating mechanism (m)
y	: Displacement of the slider (link 4) (m)

Greek Symbols

α	: Angle subtended by the crank (rad.)
β	: Pivot angle of link 3 (rad.)
ϕ	: Crank angle (rad.)
λ	: Coefficient of resistance given by Blasius formula
μ	: Dynamic viscosity of fluid (Ns/m^2)
θ	: Oscillation angle (rad.)
ρ	: Fluid (air) density (kg/m^3)
ρ_l	: Density of manometer fluid (kg/m^3)
τ	: Time variable (s)
ω	: Circular frequency of pulsation (rad./s)
ω_{bU}	: Upper bound of bursting circular frequency (rad./s)
ω_{bL}	: Lower bound of bursting circular frequency (rad./s)
ω^*	: Frequency parameter, $R(\omega/2\upsilon)^{\frac{1}{2}}$

REFERENCES

[1]. Arasi, J. 'Results Mixed From Pulsating Flow Tests of Orifice-Plate Meters.' *Oil and Gas Journal.* Oct., 1992, p.77-82.

[2]. West, F.B. and Taylor A.T. 'The Effect of Pulsations on Heat Transfer in Turbulent Flow of Water Inside Tubes.' *Chemical Engineering Progress.* Vol. 48, No. 1, 1952 p. 39 - 43.

[3]. Karamercan, O.E. and Gainer, J.L. 'The Effect of Pulsation on Heat Transfer' *Industrial Engineering Chem. Fund.* Vol. 18, No. 1, 1979. p. 11-15

[4]. Liao N.S. and Wang C.C. 'An Investigation of Heat Transfer in Pulsating Turbulent Pipe Flow.' *Fundamentals of Forced and Mixed Convection*, The 23rd National Heat Transfer Conference. Denver, Co. U.S.A, Aug. 4-7, 1985, p. 53-59.

[5]. Mamayev, V.V., Nosov, V.S and Syromyatnikov, N.I. 'Investigation of Heat Transfer in Pulsed Flow of Air in Pipes.' *Heat Transfer - Soviet Research*, Vol. 8, No. 3, 1976, p. 111-116.

[6]. Babus'haq, R.F. 'Forced Convection Heat Transfer in The Entrance Region of Pipes.' *International Journal of Heat and Mass Transfer*, Vol. 36, No. 13, 1993, p. 3343-3349.

[7]. Sparrow, E.M., Hallman, T.M. and Siegel, R. 'Turbulent Heat Transfer in The Thermal Entrance Region of a Pipe with Uniform Heat Flux.' *Applied Science Research*, ser. A, Vol. 7, 1957, p. 37-52.

[8]. Kays, W.M .and Crawford, M.E. 'Convective Heat and Mass Transfer. 2nd. Ed. *McGraw-Hill Book Co.*, New-York. U.S.A. 1980.

[9]. Hussain, A.K.M.F. 'Mechanics of Pulsatile Flows in Relevance to Cardiovascular Systems.' *In Cardiovascular Flow Dynamics and Measurements* (Ed. N.H.C Hwang and N.A Normann) Baltimore Univ. Park Press. 1977.

[10]. Martinelli, R.C., Boelter, L.M.K., Weinberg, E.B. and Yakahi, S. 'Heat Transfer to a Fluid Flowing Periodically at Low Frequencies in a Vertical Tube.' *Transaction of ASME*, Oct. 1943, p. 789-798.

[11]. Havemann, H.A. and Rao, N.N. 'Heat Transfer in Pulsating Flow.' *Nature.* Vol. 7, No. 4418. 1954, p. 41.

[12]. Lemlich, R. 'Vibration and Pulsation Boost Heat Transfer.' *Chemical Engineering*, May, 1961, p. 171-176.

[13]. Lemlich, R. and Hwu, C. 'The effect of Acoustic Vibration on Forced Convective Heat Transfer' *A.I.Ch.E. Journal*, Vol. 7, No.1, 1961, p. 102-106.

[14]. Baird, M.H.I, Duncan, G.J., Smith, J.I and Taylor, J. 'Heat Transfer in Pulsed Turbulent Flow.' *Chemical Engineering Science*. Vol. 21, 1966, p. 197-199.

[15]. Genin, L.G., Koval, A.P., Manchkha, S.P. and Sviridov, V.G. 'Hydrodynamics and Heat Transfer with Pulsating Fluid Flow in Tubes.' *Thermal Engineering*, Vol. 39, No.5, 1992, p. 30-34.

[16]. Al-Haddad, A. and Al-Binally, N. 'Prediction of Heat Transfer Coefficient in Pulsating Flow.' *International Journal of Heat and Fluid Flow*. Vol. 10, No. 2. 1989, p. 131-133.

[17]. Isshiki, S., Obata, T., Kasagi, N., Hirata, M. 'Experimental Study on Heat Transfer in a Pulsating Pipe Flow.' *Nippon Kikai Gakkai Ronbunshu, B Hen / Trans. J.S.M.E*, Part B, Vol. 59, No. 563, 1993, p. 145-151.

[18]. Siegel, R. and Perlmutter, M. 'Heat Transfer For Pulsating Laminar Duct Flow.' *Journal of Heat Transfer*, May, 1962, p. 111-123.

[19]. Faghri, M., Javdani, K. and Faghri, A. 'Heat Transfer with Laminar Pulsating Flow in a Pipe.' *Letters in Heat and Mass Transfer*, Vol. 6, No. 4, 1979, p. 259-270.

[20]. Siegel, R. 'Influence of Oscillation Diffusion on Heat Transfer in a Uniformly Heated Channel.' *Journal of Heat Transfer*, Vol. 109, 1987, p. 244-247.

[21]. Cho, H.W. and Hyun, J.M. 'Numerical Solutions of Pulsating Flow and Heat Transfer Characteristics in a Pipe.' *International Journal Of Heat and Fluid Flow*, Vol. 11, No. 4, 1990, p. 321-330.

[22]. Kim, S.Y., Kang, B. H. and Hyun, J. M. 'Heat Transfer in The Thermally Developing Region of a Pulsating Channel Flow.' *International Journal of Heat and Mass Transfer*, Vol. 36, No. 17, 1993, p. 4257-4266.

[23]. Ohmi, M., Osui, T., Tanaka, O. and Toyama, M. 'Pressure and Velocity Distributions in Pulsating Turbulent Pipe Flow.' *Bulletin of The Japanese Society of Mechanical Engineers*, Vol. 19, No. 134, 1976, p. 951-957.

[24]. Clamen, M. and Minton, P. 'An Experimental Investigation of Flow in an Oscillating Pipe.' *Journal of Fluid Mechanics*, Vol. 81, 1977, p. 421-431.

[25]. Carvalho, J.A. 'Behavior of Solid Particles in Pulsating Flows.' *Journal of Sound and Vibration.* Vol. 185, No. 4, 1995, p. 581-593.

[26]. Kastner, L.J and Shih, S.H 'Critical Reynolds Numbers for Steady and Pulsating Flow.' *Engineering*, Sept. 1951, p. 389-391.

[27]. Ede, A.J. 'Effect of an Abrupt Disturbance of The Flow on the Local Heat Transfer Coefficient in a Pipe.' *Heat 164*, National Eng. Lab. East Kilbride, Glasgow Scotland, 1959.

[28]. Zemanick, P.P. and Dougall, R.S. 'Local Heat Transfer Downstream of Abrupt Circular Channel Expansion.' *Journal of Heat Transfer*, Feb., 1970, p. 53-60.

[29]. Habib, M.A., Mobarak, A.M., Attya, A.M. and Aly, A.Z. 'Enhanced Heat Transfer in Channels with Staggered Fins of Different Spacings.' *International Journal of Heat and Fluid Flow*, Vol.14, No. 2, 1993, p.185-190.

[30]. Edwards, R.J., Jambunathan, K. and Button B.L. 'Experimental Investigation of Turbulent Heat Transfer in Simultaneously Developing Flow in Finned Annuli.' *Experimental Heat Transfer Fluid Mechanics and Thermodynamics*, 1988, p. 543-549.

[31]. Habib, M.A. and McEligot, D.M. 'Turbulent Heat Transfer in a Swirl Flow Downstream of an Abrupt Pipe Expansion.' *7th Int. Heat Transfer Conference, Munchen*, Paper FC29. 1982.

[32]. Yao, M, Nakatani, M and Suzuki, K. 'Flow Visualization and Heat Transfer Experiment in a Duct with an Insertion of a Staggered Array of Cylinders' *Experimental Heat Transfer Fluid Mechanics and Thermodynamics*, 1988, p. 519 -526.

[33]. Prasad, R.C. and Brown, M. J. 'Effectiveness of Wire - Coil Inserts in Augmentation of Convective Heat Transfer' *Experimental Heat Transfer Fluid Mechanics and Thermodynamics*, 1988, p. 502-510

[34]. Rao, K.N., Narassihma, R. and Narayanan, M.A.B. 'The Bursting Phenomenon in a Turbulent Boundary Layer' *Journal of Fluid Mechanics*, Vol. 48, Part 2, 1971, p. 339-352.

[35]. Mizushina, T., Maruyama, T., Shiozaki, Y. 'Pulsating Turbulent Flow in a Tube.' *Journal of Chemical Engineering, Japan*, Vol. 8, 1973, p. 210-216.

[36]. Ramaprian, B.R. and Tu, S.W. 'Fully Developed Periodic Turbulent Pipe Flow-Part 2: The detailed Structure of The Flow.' *Journal of Fluid Mechanics*, Vol. 137, 1983, p. 59 - 81.

[37]. Schlitching H. 'Boundary Layer Theory.', Seventh Edition, *McGraw-Hill Book Company*, N.Y. 1991.

[38]. Stearns, R. F., Johnson, R. R., Jackson, R. M. and Larson, C. A. 'Flow Measurements with Orifice Meters.' *D. Van Nostrand Company, Inc.*, New-York, 1951.

[39]. Roberson, J.A. and Crowe, T. 'Engineering Fluid Mechanics.' 4th Edition, *Houghton Mifflin Company*, Boston. 1990.

[40]. Holman, J. P. 'Experimental Methods for Engineers' 4th Edition. *McGraw-Hill Book Company*, New York, 1984.

VITA

- Gbadebo, Semiu Adesina.
- Born in Abeokuta, Ogun-State, Nigeria.
- Obtained a Bachelor's Degree with First Class Honors in Mechanical Engineering from Obafemi Awolowo University, Ile-Ife, Nigeria in September, 1989.
- Worked as a Teaching Assistant in the College of Engineering of Anambra State University of Technology, Enugu, Nigeria. (Nov. 1989-Oct. 1990)
- Worked as a Technical Service / Sales Engineer with Tractor & Equipment Division of UAC of Nigeria / Leverton Group UK. (Jan. 1991-Sept. 1994)
- Completed Master's Degree requirements at King Fahd University of Petroleum & Minerals, Dhahran, Saudi Arabia in December, 1996.